FINAL REPORT

National Aeronautics and Space Administration

GRANT NGR-39-005-105

ANALYSIS OF PROTON AND ELECTRON SPECTROMETER DATA FROM OGO-5 SPACECRAFT

Period: July 1, 1973 - July 31, 1974

Principal Investigator - Martin A. Pomerantz

Bartol Research Foundation
of
The Franklin Institute
Swarthmore, Pennsylvania
19081

Submitted: February 13, 1975

The results of the research performed under NASA Grant NGR-39-005-105 consist of two publications in scientific journals, and a doctoral thesis.

Dr. Erling Nielsen completed his thesis entitled "Propogation of Low Energy Solar Cosmic Rays in the Interplanetary and Geomagnetic Field" during the period of this grant. Dr. Nielsen completed his work at the Bartol Research Foundation in September, 1974, and accepted an appointment at the Max Plank Institut fur Aeronomie, Lindau, Germany.

Preprints of the publications entitled "Access of Solar Electrons to the Polar Regions" and "Angular Distributions of Solar Protons and Electrons" are appended; both papers have been accepted for publication in Planetary and Space Science. Copies of the doctoral thesis are available from the Bartol Research Foundation.

Access of Solar Electrons to the Polar Regions

E. Nielsen* and M.A. Pomerantz

Bartol Research Foundation of The Franklin Institute
Swarthmore, Pennsylvania 19081

Abstract — The interaction between the geomagnetic and interplanetary magnetic fields is studied through its effects upon the intensities of solar electrons reaching the polar caps during times of strongly anisotropic electron fluxes in the magnetosheath. During the particle event of November 18, 1968, electrons of solar origin were observed outside the magnetopause with detectors aboard OGO-5. This is the only case on record for which high resolution directional flux observations are available for determining in detail the electron angular distribution, and thus the electron density in the magnetosheath.

Correlative studies of these satellite observations and concurrent measurements by riometers and ionospheric forward scatter systems in both polar regions have revealed that the initial stage of the associated Polar Cap Absorption event is attributable to the prompt arrival of solar electrons. The electron flux precipitating into the south polar region was equal to or larger than the mean directional flux in interplanetary space, whereas over the north pole it was equal to or less than the backscattered flux. This evidence of a north-south asymmetry in the solar electron flux at a time when the interplanetary magnetic field vector was nearly parallel with the ecliptic plane supports an open magnetospheric model. The ratio of particle intensities in the

*Present address: Max Planck Institut für Aeronomie, Lindau, Germany.

High Polar Latitude and Low Polar Latitude regions in the southern hemisphere is consistent with that determined at times when the interplanetary electron fluxes were isotropic. The analysis indicates that an anisotropic electron flux may be isotropized at the magnetopause before propagating into the polar regions.

1. Introduction

The common feature of all so-called open magnetospheric models is that the geomagnetic field lines anchored at high polar latitudes are directly connected to the interplanetary magnetic field (imf) lines, thereby providing a direct path for low rigidity solar particles into the polar ionosphere (Dungey, 1961, 1965; Axford et al., 1965; Morfill and Quenby, 1971; Morfill and Scholer, 1972). The intensity of particles precipitating at each pole is related to the particle flux along the respective field lines in interplanetary space, and when this flux is anisotropic, i.e., when the intensities of particles propagating toward and away from the sun are unequal, these models predict correspondingly different intensities in the two polar caps.

Anisotropic solar proton fluxes have been used as tools in the investigation of the earth's magnetic environment (Van Allen et al., 1971; Domingo and Page, 1971). However, similar observations during periods when the interplanetary electron flux is anisotropic have never been obtained. This is a consequence of the relatively short duration (one to two hours) of appreciable anisotropy of solar electrons (Allum et al., 1971) which precludes carrying out the required measurements of the electron fluxes over both polar caps with a polar orbiting satellite prior to the decay of the anisotropy. It is of considerable interest to make simultaneous observations over the

polar caps because the magnetic field configuration in the open magnetospheric models that have been proposed allow adiabatic access of the low rigidity electrons, i.e., these particles are "good" tracers of magnetic field lines. Thus, at least in principle, such observations of access to the magnetosphere of anisotropic electron fluxes in the magnetosheath could provide a definitive test of the validity of the open models.

As emphasized by Paulikas (1974), observations of solar particle fluxes in the magnetosphere indicate that the real magnetosphere is more complex than the models imply. In particular, it appears that the solar particles have different modes of access to two regions of the polar cap, one characterized by open field lines ["High Polar Latitudes" (HPL)], the other by closed field lines ["Low Polar Latitudes" (LPL)].

In the light of observations of proton fluxes in the HPL regions during times of interplanetary proton anisotropies, one would expect to observe higher electron intensities in the HPL region over that pole which in an open magnetospheric model is magnetically connected to the sun, and lower intensities over the other pole during times of interplanetary electron anisotropies, giving rise to a north-south (NS) asymmetry.

The interaction between the incoming particles and the earth's atmosphere has the effect of enhancing the electron density in the ionosphere, which causes an increase in the attenuation of HF-radio waves propagating through the ionosphere. If the intensities of particles precipitating into the two HPL

regions differ, different attenuations result, all other factors being equal, hence observations of radio wave absorption provide a direct measure of the intensities. However, if the spectra over the two HPL regions differ, or if one region is sunlit and the other is not, it is necessary to resort to calculations in order to extract information about the intensities from the absorption observations.

The solar flare of November 18, 1968, produced a particle event characterized by very large field aligned electron anisotropies, as observed with a satellite beyond the magnetopause (Nielsen et al., 1974). The direction of the imf was near the ecliptic plane and pointing away from the sun so that the higher electron intensity was expected over the southern HPL region. In the present paper, radio wave absorption measurements at high polar latitudes in the two hemispheres, obtained with riometer and ionospheric forward scatter apparatus, are compared with absorption calculations based upon the electron energy spectra derived from satellite observations in the magnetosheath primarily to determine whether or not a NS-asymmetry in the solar electron flux occurred during this event.

2. Satellite Observations

The earth-orbiting satellite OGO-5 was located in the magnetosheath at a distance of 23.3 R_E from the earth at 1100 UT on November 18, 1968. The Lawrence Livermore Laboratory electron and proton spectrometers (West et al., 1969, 1973)

on board this satellite detected the onset of the electron event at 1045±05 UT, whereas 6 MeV protons first arrived between 1105-1145 UT (Nielsen et al., 1974). Thus the solar electrons arrived at the earth prior to these protons.

Early in the event, even after proton onset, the electron flux was much larger than the proton flux. In any event, precipitation of the higher energy protons that first reach the earth will not give rise to appreciable electron density increases in the ionosphere because most of their energy is lost by ionization deep in the atmosphere (<50 km), where the lifetime of free electrons is short. Several authors (Van Allen et al., 1964; Juday and Adams, 1969; Reid, 1969) have used the empirical relation: $\sqrt{F} = R \cdot A$, to relate the integral fluxes F of protons above some energy E_{min} to the riometer absorption A at a given frequency. R is a constant, dependent only upon E_{min}. Potemra and Lanzerotti (1971), using solar proton data from the synchronous equatorial ATS-1 satellite, deduced R as a function of E_{min} from the 30 MHz riometer absorption observed at Byrd during the January 28, 1967 event. At the time of interest during the November 18, 1968 event (1110 UT) a minimum value of the energy of protons which have arrived at the earth is $E_{min} = 46$ MeV. The corresponding R-value from Potemra and Lanzerotti (1971) is $R \approx 5.5$. At this time the 46 MeV proton flux is <0.05

proton/cm^2-sec-str-MeV, and with a typical value of 3 of the exponent in a power energy spectrum of differential intensities, we find that the proton induced riometer absorption at 30 MHz is $A < 0.2$ dB, which is the same order of magnitude as the uncertainty of riometer absorption measurements, and an order of magnitude less than the observed absorption at 1110 UT.

On the other hand, the electrons which govern the electron induced absorption during this event ($\sim$300 keV) ionize profusely at higher altitudes ($\sim$70 km) where relatively high electron densities can be maintained, owing to the decreased probability for a free electron to be attached to a neutral molecule or to recombine with a positive ion. Thus, at early times following onset, we expect the electron density in the ionosphere to be governed by the influx of solar electrons.

Comparison between measurements of isotropic interplanetary electrons with electrons in the HPL regions have revealed that they were identical with respect to both intensity and the form of the energy spectrum (West and Vampola, 1971). This indicates that a solar electron propagating into the polar caps suffers neither energy gain nor loss. For the calculations

of HF-radio wave absorption that will be compared with the observations, we will assume that the energy spectra J(E) of the electrons precipitating over the south pole are those determined for the mean directional fluxes in the magnetosheath (curves A in Figure 1), while we assume that over the north pole the electron energy spectra are determined by the mean of the directional fluxes of particles which have been backscattered beyond the orbit of the earth and propagate toward the sun (curves B in Figure 1). Since energy channels in the electron spectrometer are narrow, the channel center energies have been used in determining the spectra.

3. Radio Wave Absorption Observations

Ground-based observations of ionospheric absorption of radio waves during the November 18, 1968 particle event were obtained with Bartol's network of forward scatter systems, located at high latitudes. However, the only forward scatter link operating in the northern hemisphere at the time was suffering transmitter problems. Fortunately, the combination of forward scatter and riometer data have made it possible to carry out this analysis, nevertheless. Some aspects of the absorption experiments that are relevant to the present investigation are summarized in Table 1.

Forward Scatter. A forward scatter system comprises two stations separated by a distance of, typically, 1000 km. Identical highly directional antennas at each site are aimed

at a point in the D-layer, midway between the transmitter and receiver, where the transmitted signal suffers scattering against electron density fluctuations, as a consequence of which a small fraction of the energy reaches the receiver. The scattering efficiency is proportional to the logarithm of the ambient electron density at the scattering stratum, which during daylight at high latitudes is at an altitude of 75±2 km (Bailey et al., 1970), hence an increase in the electron density in this height interval leads to an enhancement in the received forward scatter signal. On the other hand, any increase in the ionization below the scattering stratum leads to greater absorption of the electromagnetic wave than that suffered during quiet times.

Thus, during a typical solar particle event, the received power is determined by the difference between an enhancement effect caused by the electron density increase at an altitude of ∿75 km and an absorption effect resulting from the increase in ionization below that altitude.

The forward scatter records from Byrd-McMurdo (BM), representative of conditions in the Antarctic HPL-region, is reproduced in Figure 2a. The absorption started at ∿1050 UT, and continued to increase until 1110 UT. The received signal intensity then remained nearly constant for about 5 minutes, until 1115 UT when a second onset, which is attributable to the arrival of solar protons, occurred. Thus, the absorption before 1115 UT was governed by solar electron precipitation. The absorption between 1110 UT and 1115 UT was 26.5 dB; the uncertainty in es-

timating the signal enhancement together with the limited accuracy in determining the signal level from the records combine to produce an uncertainty in the absorption observation of ±2 dB.

The forward scatter absorption in the LPL-region is represented by Figure 2b, which shows the signal intensity in Byrd-South Pole link. The absorption in the above mentioned time interval was 14.5±2 dB. During times of isotropic interplanetary fluxes the intensity of electrons precipitating into the LPL region has been found to be a function of magnetic local time (Vampola, 1971). We note for later use that the above absorption measurements were made at ~0600 magnetic local time.

Riometer. (a) Antarctic measurements: The cosmic noise decrease produced by solar x-rays commenced at 1026 UT, reached a maximum at 1050 UT and ended at 1220 UT (Lincoln, 1970). Figure 3a shows the absorption measured at McMurdo, which is located in the HPL region. Since the absorption measured prior to the time of the solar radio frequency burst is induced solely by x-rays, as represented by the dashed line in Figure 3a, the contribution must be subtracted to determine the absorption produced by charged particles only. Between 1110 UT and 1120 UT, the absorption induced by precipitating solar electrons was 2 dB. Thereafter, the absorption increased rapidly owing to the arrival of low energy solar protons.

(b) Arctic measurements: Figure 3b shows the record ob-

tained with the 30 MHz riometer at Shepherd Bay. Clearly, the absorption at this station before 1130 UT was ≤0.2 dB. The 30 MHz riometer observations at Thule indicate onset at 1055 UT, 0.1±0.1 dB absorption at 1120 UT and 0.2 dB at 1300 UT (Ray Cormier, private communication), i.e., before proton onset the upper limit of the absorption at Thule and Shepherd Bay, both located inside the polar plateau, was 0.2 dB.

Summary. On November 18, 1968, the ionospheric forward scatter absorption in the BM-path before 1115 UT and the riometer absorption at McMurdo before 1120 UT reflect the intensity of electrons precipitating into the southern polar plateau, i.e., the HPL region in Antarctica which may be magnetically linked to interplanetary space. The difference between the above times arises from the fact that the forward scatter system is more sensitive than the riometer (especially to the high energy protons, which arrive earliest). Thus, at 1110 UT the forward-scatter and riometer absorptions for Antarctica, which are relevant for an investigation of North-South asymmetry, were 26.5 dB and 2.0 dB, respectively. In the corresponding region in the northern polar cap the riometer absorption was ≤0.2 dB.

4. Theoretical Model of Radio Wave Absorption

Electron Density Profile. In order to determine the altitude profile of electron density $n_e(h)$ created by the solar electrons, it is first necessary to calculate the ionization rate $q(h)$ (number of electrons produced per cm^3/sec) as a func-

tion of altitude h.

Spencer's (1959) tabulation of the electron energy loss by collisional ionization, in terms of the residual ranges of the incident electrons, provides the basis for this calculation (Nielsen, 1974). Both nuclear elastic scattering and electron slowing down due to collisions are taken into account. The effect of range straggling arising from large discrete energy losses suffered in both radiative and inelastic collisions is considered to be negligible. The CIRA (1965) atmospheric model, and collision frequencies listed by Bailey et al. (1970), were adopted for carrying out the computations.

The electrons and ions produced by the precipitating solar electrons will seek equilibrium with the medium in which they are produced. It is expedient to ignore the detailed chemical reactions that take place between the constituents of the atmosphere, and to treat the reactions collectively in terms of effective or macroscopic reactions represented by an effective recombination coefficient α_{eff} (LeLevier and Branscomb, 1968), defined under steady state conditions as: $\alpha_{eff}(h) = q(h)/n_e^2(h)$.

We reiterate here that the purpose of this study is to establish whether or not there was a north-south asymmetry, with the greater flux over the south pole. In order to answer this question we will determine two extrema: (1) the minimum flux that is consistent with the absorption measurements in Antarctica, and (2) the maximum flux that is consistent with

the absorption recorded in the northern polar area. If (1) exceeds (2), an asymmetry occurred.

It is clear that the minimum value of α_{eff} yields the maximum value of n_e, and hence the maximum calculated absorption. Thus, by adjusting the flux of precipitating electrons so that the calculated and observed absorptions are equal, we determine the minimum value of the flux. Conversely, the upper limit on the flux corresponds to the upper limit of α_{eff}. Thus for calculations of absorptions in the southern and northern polar areas we will assume the lower and upper limits of α_{eff}, respectively.

In the sunlit hemisphere (in this case Antarctica), where the solar ultraviolet radiation produces a high rate of electron detachment from negative ions, the detachment rate is much higher than the ion-ion recombination rate, which implies that, at any given altitude, α_{eff} is a constant characterizing the atmosphere independent of the positive ion density n_+. Figure 4 shows two altitude proviles of the daytime effective recombination coefficient. One (Potemra et al., 1969) was determined by comparing proton flux measurements in space with riometer and VLF observations of seven events. The other (Bailey et al., 1970) was based upon auroral observations (altitudes above 83 km) and measured proton energy spectra during the hard, early stages of a Polar Cap Absorption (PCA) event (lower altitudes) in conjunction with riometer observations.

In the dark hemisphere (in this case the Arctic), the

ion-ion recombination resulting from an increase in the negative ion density cannot be neglected, and α_{eff} is a function of the concentration of positive ions, i.e., it depends upon the intensity and energy spectrum of the precipitating solar flare particles. If n_+ increases above the quiet time level, as it does during a solar particle event, then α_{eff} decreases, thereby increasing the equilibrium electron density above that corresponding to values of α_{eff} representative of the quiet ionosphere (Figure 4). Zmuda and Potemra (1972) determined the nighttime altitude profile of α_{eff} for the event of February 25, 1969, for which the production rate at altitudes above 62 km is larger than that determined in the present study for the November 18, 1968, event. In light of the earlier comments, it now follows that α_{eff} during the November 18, 1968 event must have been less than, but perhaps close to the values valid for the February 25 event for which the corresponding α_{eff} altitude profile is shown in Figure 4. In our estimate of flux over the northern polar area we will use this α_{eff} profile for altitudes $\geq$62 km and the α_{eff} representing the quiet ionosphere below 62 km.

Figure 1 indicates that between 1110 UT and 1120 UT, the precipitating solar electron flux was only slowly varying compared to the <100 sec average lifetime of the various species of positive ions (Bailey et al., 1970). It takes a certain time for the ionosphere to reach equilibrium after exposure to a given ionizing agent, as represented by a time constant $\tau \simeq 1/(2\ \alpha_{eff}\ n_e)$. Calculations of n_e during the early stage of the event (Nielsen,

1974), show that at night $\tau \approx 1$ sec, whereas $\tau \approx 1$ min during the day. We consider this to be justification for the approximation that between 1110 and 1120 UT the ionosphere reached equilibrium almost instantaneously after the influx of solar electrons. Thus, in terms of the ionization rate and effective recombination coefficient, the equilibrium electron density is well determined by an expression that is valid under steady state conditions.

Absorption. Radio wave absorption is computed using the work of Sen and Wyller (1960), who calculated the complex refractive index of a weakly ionized gas in a steady magnetic field. Their model takes into consideration the fact that the collision frequency of electrons with neutral particles is a function of electron velocity.

Since the magnetic field lines in the polar caps are nearly vertical, the cosmic noise signal detected by a riometer with an ideal vertical pencil beam antenna has propagated parallel with the magnetic field, i.e. longitudinal propagation. On the other hand, in the forward scatter systems, the zenith angle of the signal paths is nearly 85°, hence propagation is essentially transverse.

The calculated absorption equals that which would have been observed if the antennas had an ideal pencil beam gain pattern. A typical riometer has a broad-beam antenna, and this leads to a further increase in the observed absorption above that which would have been expected for a pencil beam antenna.

Assuming that the ionization is homogeneous over the part of the ionosphere which affects the riometer signal, Eklund and Hargreaves (1968) found that the absorption increases by a factor 1.4. Furthermore, a riometer antenna responds equally well to the ordinary and extraordinary components of the cosmic noise signal, and Bailey (1968) showed that this further increases the observed absorption by a factor 1.11.

In contrast with the riometer, the geometric properties of ionospheric forward scattering (the scattering takes place in an effective region around the path-midpoint with dimensions of the order of 100 km), make it unnecessary to apply any substantial correction to the calculated absorption for a pencil beam antenna (Bailey et al., 1955). The correction for the ordinary component is of the order of 1 percent and has been neglected (Bailey et al., 1970). Consequently, no substantial correction of the calculated absorption is required in this case, and the calculated and observed absorptions can be compared directly.

5. Comparison of Observed and Predicted Absorptions

Observations in the LPL and HPL Regions in the Southern Hemisphere. The absorption in the Byrd-South Pole path A_{BS} prior to the onset of proton induced absorption was about half of that in the Byrd-McMurdo path A_{BM}. Corrections for differences in path length and radio wave frequency increase the ratio A_{BS}/A_{BM} to approximately 0.65. For a given form of the

energy spectrum the daytime absorption at the high frequencies utilized in this study is approximately proportional to the square root of the integrated flux. Assuming (1) that the spectral shapes in the LPL region and in the HPL region are the same (as is the case when the interplanetary electron flux is isotropic, Vampola, 1971) and (2) that the cutoff rigidity at the midpoint of the Byrd-South Pole path is so low as to not significantly influence the absorption (the cutoff, 10 keV for electrons, is $\sim 10^5$ V), then the integrated flux, and thus the flux in a given energy interval in the Byrd-South Pole path (LPL-region) is about $(0.65)^2$ or roughly 40% of that in the Byrd-McMurdo path (HPL-region). This is in very good agreement with measurements made during times of isotropic interplanetary fluxes as represented in Figure 5, which shows that the flux of 300 keV electrons in the LPL region (Vampola, 1971) was about 30% of that in the HPL region at 0600 h magnetic local time, approximately the time of our observations. Thus we find that during times of anisotropic interplanetary electron fluxes the ratio between the fluxes in the LPL- and HPL- region is comparable with that found when the interplanetary electron fluxes are isotropic.

North-South Asymmetry. (a) Antarctic: The observed and calculated riometer and forward scatter absorptions, representing conditions over Antarctica at early times following onset of the particle event on November 18, 1968, are listed in Table 2.

For the riometer at McMurdo the results are in good agreement. The observed FS-absorption at the midpoint of the BM-path at 1110 UT is consistent with the value calculated with the α_{eff} of Potemra et al. (1969), whereas the α_{eff} of Bailey et al. (1970) yields a value that is too low to account for the observations. Thus, the Potemra-profile provides results that agree with the observations if the calculations are based upon spectra J(E) (Section 2) determined from the mean directional fluxes observed at this time.

On the other hand, for the Bailey α_{eff} profile to lead to a calculated FS absorption that agrees with the measurements without changing the calculated riometer absorption, an electron spectrum that is harder than J(E) is required. This would increase the ionization below the scattering height and decrease it above, in such a way as to increase the FS absorption without affecting the predicted riometer absorption. However, hardening of the spectrum would imply the operation of a mechanism for accelerating solar particles in the magnetosphere, a phenomenon that has not been observed. We therefore conclude that, for the present purposes, the Potemra-profile is closer to reality than the Bailey-profile, and that J(E) is indeed the spectrum of the electrons precipitating over Antarctica at 1110 UT on November 18, 1968.

At any rate, among the reported α_{eff} profiles that of Potemra yields a minimum value for the flux precipitating over the south polar area, and is thus the relevant one for our purposes.

At 1120 UT the observed FS-absorption was larger than the calculated value for incoming electrons. This discrepancy is attributable to onset of proton precipitation at about 1115 UT.

The foregoing analysis leads to the conclusion that the electron spectrum at the top of the atmosphere over the southern polar cap was consistent with that of the mean directional flux observed in interplanetary space. In the preceding subsection, it was shown that the ratio of the fluxes in the HPL region and in the LPL region, as deduced from the absorption observations, was in accord with that observed when the interplanetary electron fluxes were isotropic. These observations, at discrete geographical locations, of electron fluxes over the high latitude areas are consistent with the interpretation that the spatial distribution of fluxes over the south polar region is independent of whether the interplanetary electron fluxes are isotropic or anisotropic. This suggests that the anisotropic flux may have been isotropized, probably at the magnetopause, before propagating to the south polar cap.

(b) Arctic: Calculations corresponding to Arctic nighttime conditions were based upon an effective recombination coefficient representing the quiet ionosphere at altitudes <62 km, whereas for higher altitudes the effects upon α_{eff} of the increase in ionization were taken into account. The predicted riometer absorption in the Arctic that would be produced by the same incoming flux as that which fits the Antarctic riometer

observations at 1110 UT and 1120 UT on November 18, 1968, is 0.42 dB. However, the maximum value of the observed riometer absorption is 0.2 dB. It is therefore necessary to reduce the intensity assumed in the calculations by a factor $\lesssim \left(\frac{0.42}{0.2}\right)^2 \gtrsim 4$.

Discussion. In open magnetospheric models, only the backscattered flux has access to the northern polar cap. The calculated values of expected riometer absorption over the north pole that would be produced by the observed backscattered flux at 1110 UT and 1120 UT (Figure 1, curves B) are 0.30 dB and 0.37 dB, respectively. Since the observed absorption in the Arctic was $\lesssim$0.2 dB, we conclude that the total flux precipitating over the north pole was even less than the backscattered flux.

In the calculations of the ionization rate, backscattering effects (i.e., scattering of solar electrons out of the atmosphere) were not specifically considered. Spencer (1959) did include backscattering in his calculations of the dissipation function for the plane perpendicular case, i.e., when the ionizing electrons penetrate into the atmosphere normally. However, in our calculations and in the actual case electrons are incident at all angles between 0° and 90°, and one would expect that the probability for an electron to backscatter is greater when it subtends a small angle (i.e., is incident nearly parallel) with the top of the atmosphere than when it arrives vertically. Because this dependence of backscattering

upon the angle of incidence has not been taken into account in the calculations representing either hemisphere, our computations probably yield too high a value for HF radio-wave absorption produced by a given incident isotropic flux. Thus, the possibility that the flux was larger than the mean directional flux in interplanetary space cannot be ruled out, since this could, in principle, account for the absorption observed over the south pole. Consequently, adiabatic access cannot be excluded. If access into the polar cap were adiabatic, the flux into the atmosphere over the Antarctic would be roughly equal to the field aligned flux in interplanetary space (i.e., about a factor 4 larger than J(E), since the particles would propagate in a manner such as to conserve their magnetic moment (first adiabatic invariant). Because the magnetic field increases from interplanetary space to the polar caps by a factor $\sim 10^4$, only electrons with pitch angle $\theta \lesssim 1°$ would reach the polar atmosphere.

Zmuda and Potemra (1972) compared calculated and observed 30 MHz riometer absorptions for 30 different cases of solar proton precipitation into the polar caps. From this we can evaluate the accuracy of the calculated absorption values. The mean value of the differences between the observed and calculated absorptions in percent of the calculated absorption $(A_{OBS}-A_{CALC})/A_{CALC}$, for these 30 cases is about 30% and the standard deviation of the differences is of the same order. Thus, an observed absorption which is a factor between 1 and

1.6 times that calculated for a given flux is consistent with the calculation within a confidence level of 66%. Within this degree of uncertainty the smallest flux $J_s(E)$ (with a spectrum of the same form as J(E) that is consistent with the observed 2 dB absorption at the south pole is smaller than J(E), by a factor $(1.6)^2 = 2.56$, i.e., $J_s(E) \geq 0.39\ J_o$. On the other hand, the largest flux $J_N(E)$ that is consistent with the upper limit on the absorption at the north pole is smaller than J(E) by a factor $(0.42/0.20)^2 = 4.4$, i.e., $J_N(E) \leq 0.23\ J_o$. Thus, taking into account the uncertainties in the calculations, we still find that the flux over the southern polar cap is larger than that over the northern by at least a factor 1.7.

All of these considerations lead to the conclusion that a north-south electron asymmetry has actually been observed for the first time.

6. Conclusions

Our analysis of satellite measurements of solar electron fluxes in the magnetosheath during the early phase of the November 18, 1968 event, together with indirect observations of the intensity of solar electrons precipitating into the earth's polar caps deduced from concurrent ground-based observations, has led to the following conclusions:

1. The electron onset in interplanetary space and the onset of High-Frequency radio wave absorption were essentially simultaneous, hence the initial stage

of the PCA is attributable to the arrival of solar electrons.

2. A north-south asymmetry of electrons occurred, and the flux over the southern polar area was $\gtrsim 1.7$ times that in the Arctic.

3. The flux precipitating over that pole which in an open magnetospheric model is magnetically connected to the sun (the south pole in this case) was equal to or larger than the mean unidirectional intensity of electrons observed in interplanetary space.

4. The flux required to produce the observed absorption over the north pole was equal to or less than the backscattered flux.

5. The ratio between fluxes in the LPL- and HPL-region in Antarctica during a period of solar electron anisotropy in interplanetary space is consistent with that observed when isotropy prevails.

All of these results are consistent with the concept of an open magnetospheric model, and with the conclusion that an interplanetary anisotropic electron flux may be rendered isotropic at the magnetopause.

Acknowledgements — We are grateful to S.P. Duggal and E.H. Levy for several helpful discussions, and to A. Masley for supplying riometer data from McMurdo and Shepherd Bay. This research was supported by NASA Grant 39-005-105. The observations in Antarctica were obtained by the National Science Foundation U.S. Antarctic Research Program.

Table 1

Ground-based HF-radio-wave experiments.

	Transmitter Location	Receiver Location	Polar Cap Region	Symbol	Frequency MHz
Forward	Byrd	McMurdo	HPL	BM	23.28
Scatter	Byrd	South Pole	LPL	BS	23.40
		McMurdo	HPL		30
Riometer		Shepherd Bay	HPL		30
		Thule	HPL		30

Table 2

Observed and calculated riometer and forward scatter absorption (in dB) in Antarctica on November 18, 1968.

Time		1110 UT	1120 UT	
Calculated	FS	18.3	19.3	α_{eff} Bailey et al. (1970)
	RIO	1.8	1.9	
	FS	24.2	22.6	α_{eff} Potemra et al. (1969)
	RIO	2.0	2.0	
Observed	FS	25.5	30.5	Byrd-McMurdo
	RIO	2.0	2.1	McMurdo

FIGURE CAPTIONS

Fig. 1 Electron energy spectra at early times during the November 18, 1968, solar cosmic ray event. Curves A are the spectra of the mean directional fluxes as observed by OGO-5 in the magnetosheath, while curves B are the mean spectra of electrons propagating toward the sun, i.e. of the mean flux of back-scattered electrons.

Fig. 2 The intensity (in dB) vs time record for two forward scatter systems. When the transmitter is turned off for about 5 minutes every half hour, the receiver functions as a riometer, recording cosmic noise. A Sudden Ionospheric Disturbance (SID) commenced at 1026 UT (Lincoln, 1970). However, the average power received in both forward scatter systems was constant between 1026 UT and the time of onset of absorption owing to particle precipitation, with the exception of the spike in the BS-record at 1046 UT. This indicates that the enhancement and absorption effect just balanced each other, and we therefore assume that the x-ray flux did not significantly affect the forward scatter signal during the particle event. A solar rf intensity enhancement lasting about 5 minutes commenced at 1046 UT, and this is probably the cause of the peak in the BS-signal. Only the receiving

antenna in the BS-link had a gain which was different from zero in the direction of the sun at this time, and that is the reason for the absence of a peak in the BM-signal.

(a) Represents the pre-event reference level of the signal, (b) the estimated enhanced level of the signal between 1110 UT and 1115 UT that would have been observed in the absence of absorption below the scattering stratum, (c) the signal intensity in the above mentioned time interval. The differences between (b) and (c) are about 26.5 dB and 14.5 dB for the BM-path and BS-path, respectively, and represent the estimated absorption of the forward scatter signals.

Fig. 3 (a) The intensity vs time records for an Antarctic riometer and (b) the absorption vs time profile for an Arctic riometer, during the event of November 18, 1968. The three horizontal bars shown in (a) indicate times during which the magnetic field in the magnetosheath had a northward component. The two earliest intervals are characterized by decreases in the absorption, indicating that a northward field prohibits proton access to the magnetosphere. The third occurs at the time of maximum absorption, which might have been larger if the field had been directed southward.

Fig. 4 Altitude profiles of the effective recombination coefficient α_{eff} for daytime and nighttime conditions. Because the production rate above ~60 km during the event of February 25, 1969, was less than that at 1110 UT on November 18, 1968, the α_{eff}-values at altitudes above ~60 km are larger than those expected on November 18, 1968. Thus utilizing α_{eff}-values corresponding to the event of February 25, 1969 for the present purposes will lead to too large a value for the calculated intensity of electrons precipitating over the Arctic region.

Fig. 5 During times of isotropic solar electron fluxes in interplanetary space, Vampola (1971) found that the solar electron fluxes formed a polar plateau (HPL region) with constant intensity, and at lower latitudes a quasi-trapping region (LPL region) where the intensity was less than 50% of that in the HPL region and varied with magnetic local time. In the figure $J_\perp$ is the flux perpendicular to the field lines in the LPL region [$J_\perp$(LPL)] and in the HPL region [$J_\perp$(HPL)], and the curve is a least-squares linear fit to data in which the points are the ratio $J_\perp(LPL)/J_\perp(HPL)$ for 312±27 keV electrons, plotted as a function of magnetic local time (Vampola, 1971). The data point denoted by a cross is determined in this study.

REFERENCES

Allum, F. R., Rao, U. R., McCracken, K. G., and Palmeira, R. A. R. (1971). Solar Phys. 17, 241.

Axford, W. E., Petchek, H. E., and Siscoe, G. L. (1965). J. Geophys. Res. 70, 1231.

Bailey, D. K., Bateman, R., and Kirby, R. C. (1955). Proceedings of the IRE 43, 1181.

Bailey, D. K. (1968). Rev. of Geophys. 70, 5823.

Bailey, D. K., Brown, R. R., and Rees, M. H. (1970). J. Atm. Terr. Phys. 32, 149.

Domingo, V., and Page, D. E. (1971). J. Geophys. Res. 76, 8159.

Dungey, J. W. (1961). Phys. Rev. Letters 6, 47.

Dungey, J. W. (1965). J. Geophys. Res. 70, 1753.

Eklund, W. L., and Hargreaves, J. K. (1968). J. Atm. Terr. Phys. 30, 265.

Juday, R. D. and Adams, G. W. (1969). Planet. Space Sci. 17, 1313.

LeLevier, R. E., and Branscomb, L. M. (1968). J. Geophys. Res. 73, 27.

Lincoln, V. (1970). WDC-A, Report UAG-9, 26.

Morfill, G., and Quenby, J. J. (1971). Planet. Space Sci. 19, 1541.

Morfill, G., and Scholer, M. (1972). Planet. Space Sci. 20, 2113.

Nielsen, E. (1974). Ph.D. Thesis at Thomas Jefferson University, July, 1974.

Nielsen, E., Pomerantz, M. A., and West, H. I., Jr. (1974). To be published.

Paulikas, G. A. (1974). Rev. Geophys. Space Phys. 12, 117.

Potemra, T. A. and Lanzerotti, L. J. (1971). J. Geophys. Res. 22, 5244.

Potemra, T. A., Zmuda, A. J., Haave, C. R., and Shaw, B. W. (1969). J. Geophys. Res. 74, 6444.

Reid, G. C. (1969). Planet. Space Sci. 17, 731.

Sen, H. K., and Wyller, A. (1960). J. Geophys. Res. 65, 3931.

Spencer, I. V. (1959). National Bureau of Standards Monograph 1.

Vampola, A. L. (1971). J. Geophys. Res. 76, 36.

Van Allen, J. A., Fennell, J. F., and Ness, N. R. (1971). J. Geophys. Res. 76, 4262.

Van Allen, J. A., Lin, W. C. and Leinbach, H. (1964). J. Geophys. Res. 69, 4481.

West, H. I., Jr., Wuject, J. H., McQuaid, J. H., Jenson, N. C., D'Arcy, R. G., Jr., Hill, R. W., and Gogdanowicz, R. M. (1969). Lawrence Radiation Laboratory, Report UCRL-50572.

West, H. I., Jr., and Vampola, A. L. (1971). Phys. Rev. Letters 26, 458.

West, H. I., Jr., Buck, R. H., and Walton, J. R. (1973). Lawrence Livermore Laboratories, Report UCRL-51385.

Zmuda, A. J., and Potemra, T. A. (1972). Rev. Geophys. Space Sci. 10, 981.

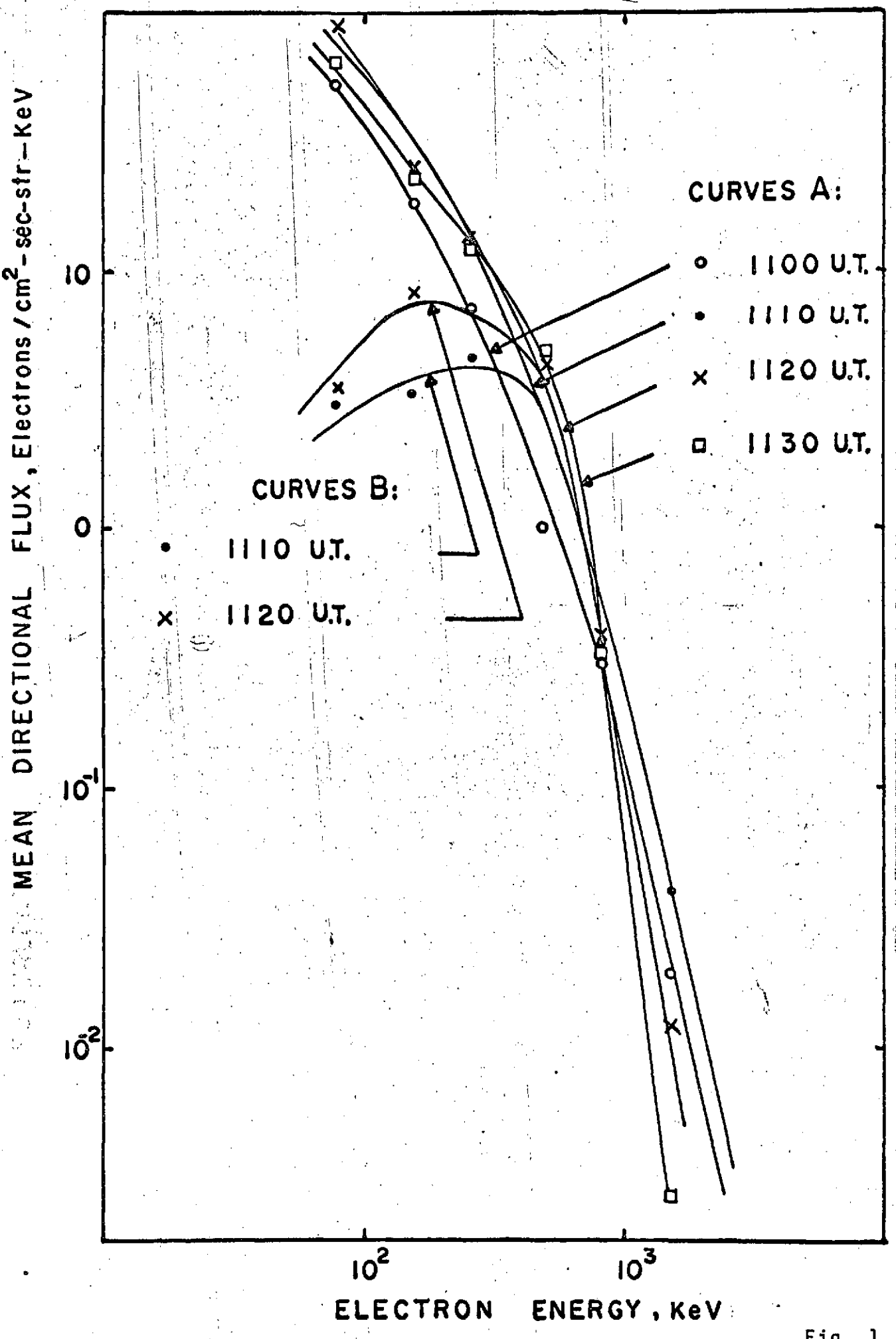
MEAN DIRECTIONAL FLUX, Electrons/cm²-sec-str-KeV
10
0
10⁻¹
10⁻²
CURVES A:
1100 U.T.
1110 U.T.
1120 U.T.
1130 U.T.
CURVES B:
1110 U.T.
1120 U.T.
10²
10³
ELECTRON ENERGY, KeV

Fig. 1

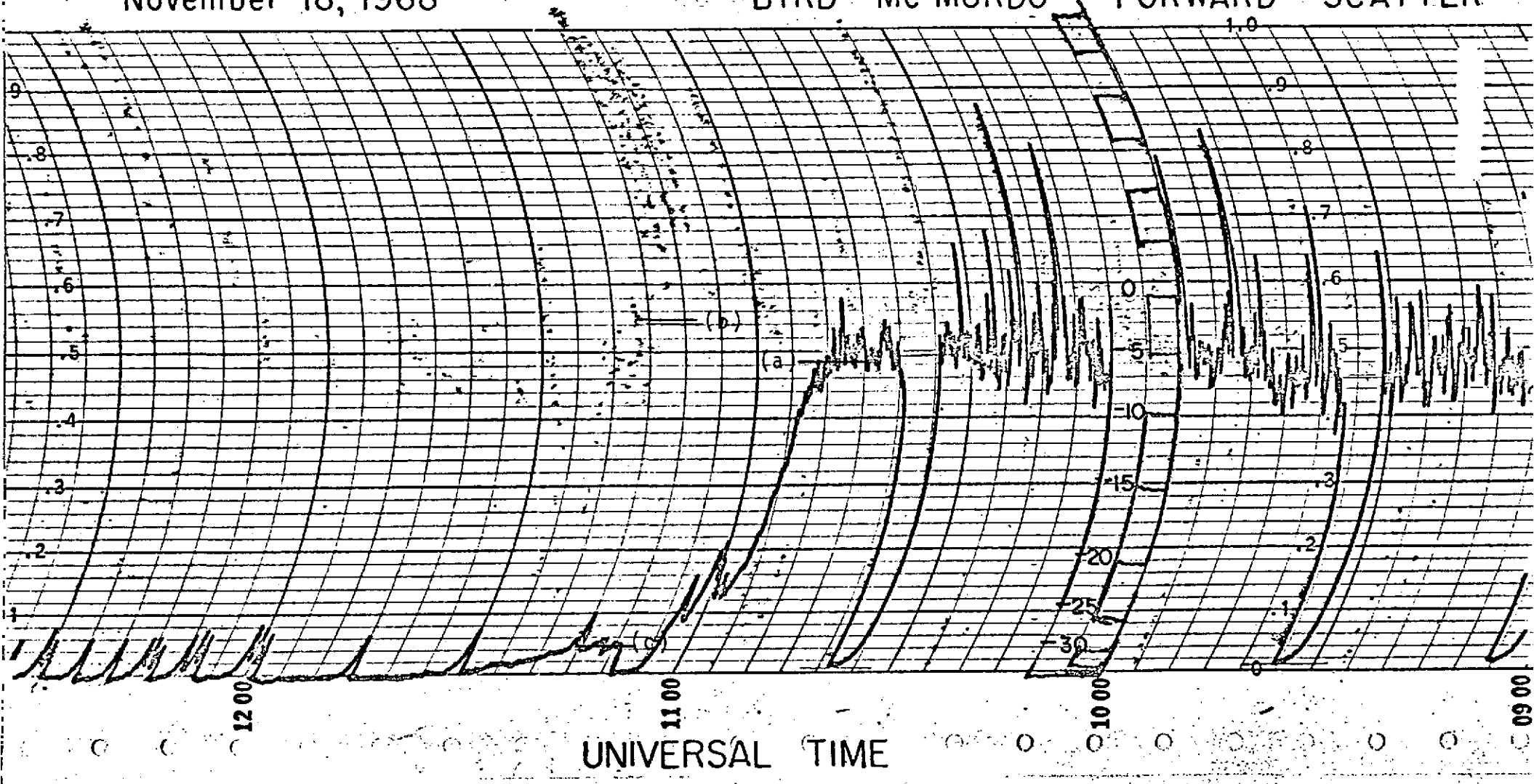

Fig. 2a

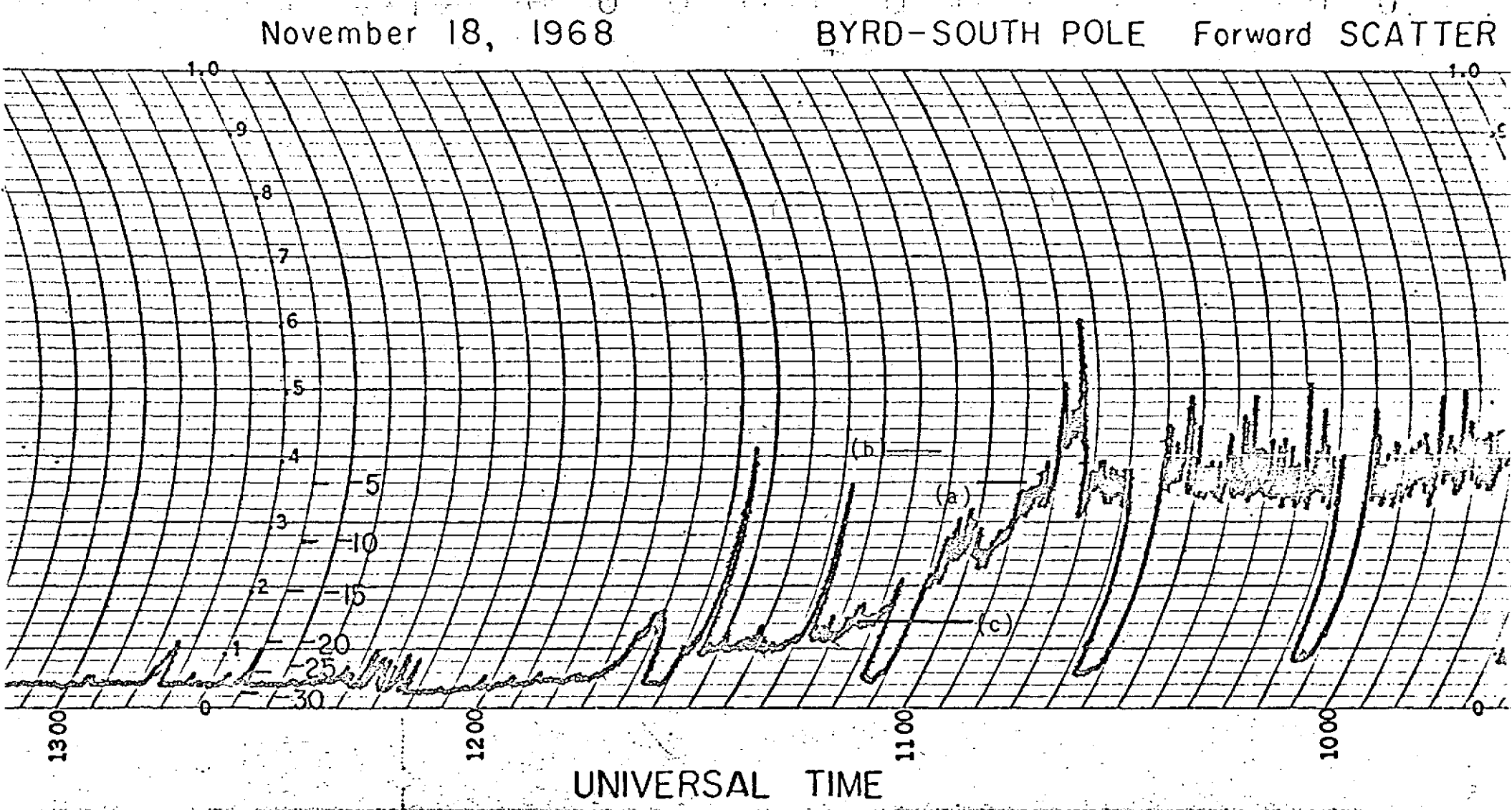

Fig. 2b

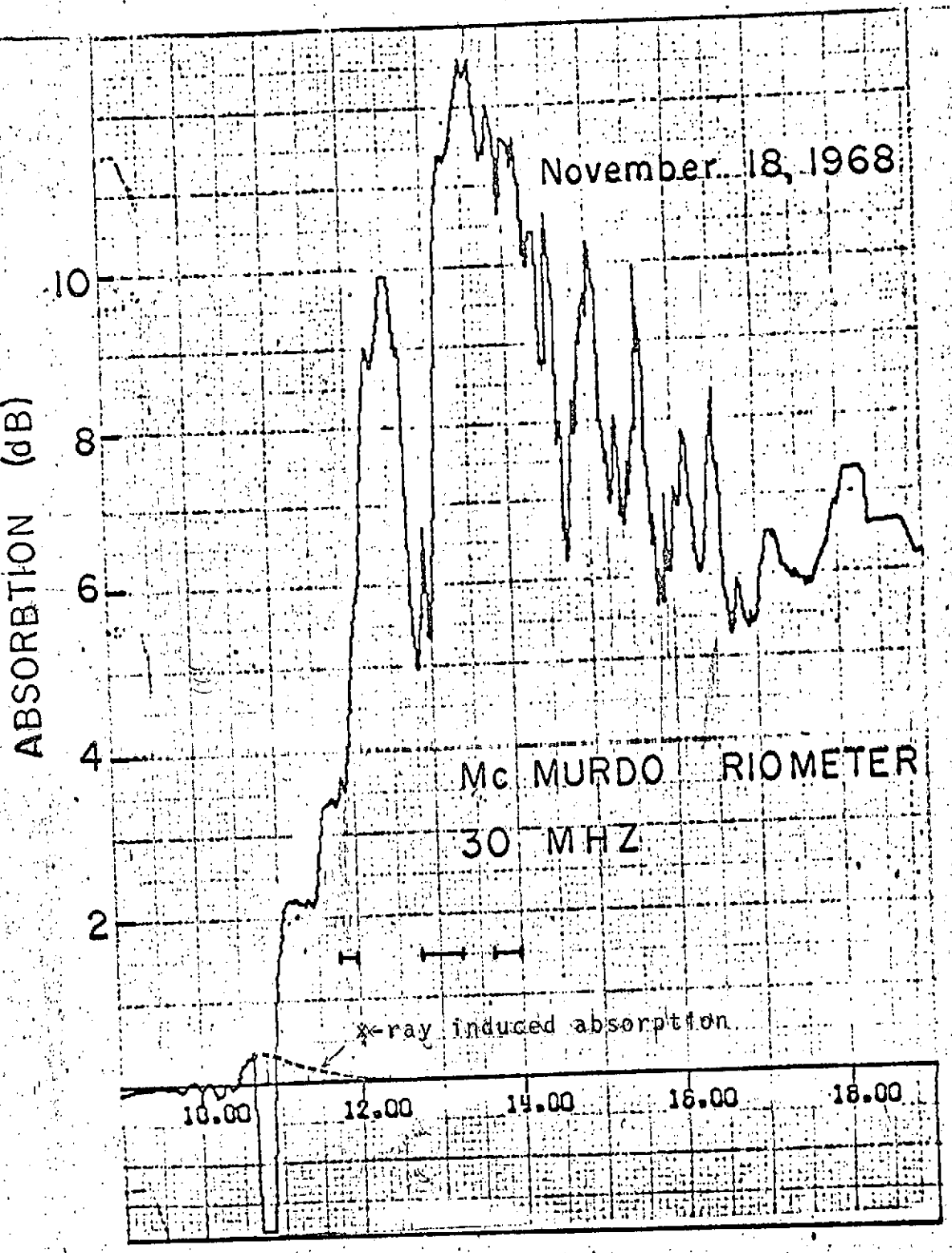
November 18, 1968
ABSORBTION (dB)
10
8
6
4
2
Mc MURDO RIOMETER
30 MHZ
X-ray induced absorption
10.00
12.00
14.00
16.00
18.00
UNIVERSAL TIME

Fig. 3a

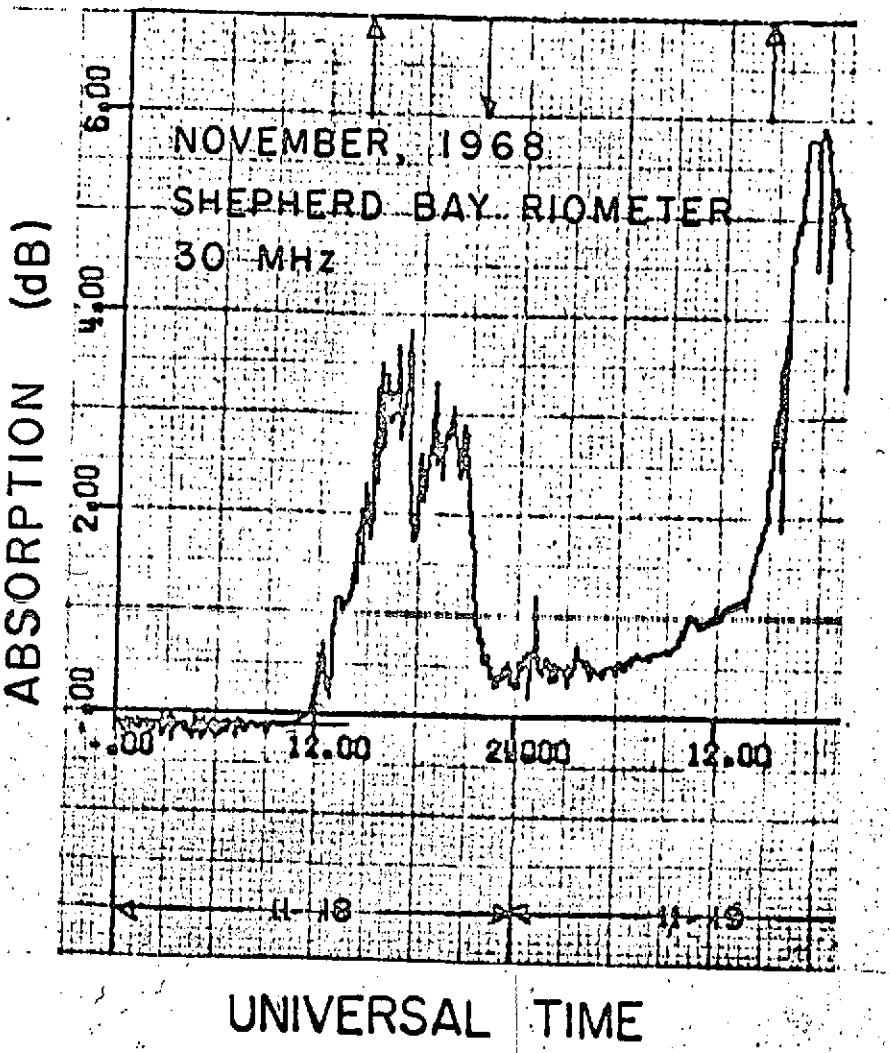
NOVEMBER, 1968
SHEPHERD BAY RIOMETER
30 MHz
ABSORPTION (dB)
6.00
4.00
2.00
1.00
.00
12.00
24.00
12.00
H-18
H-19
UNIVERSAL TIME

Fig. 3b

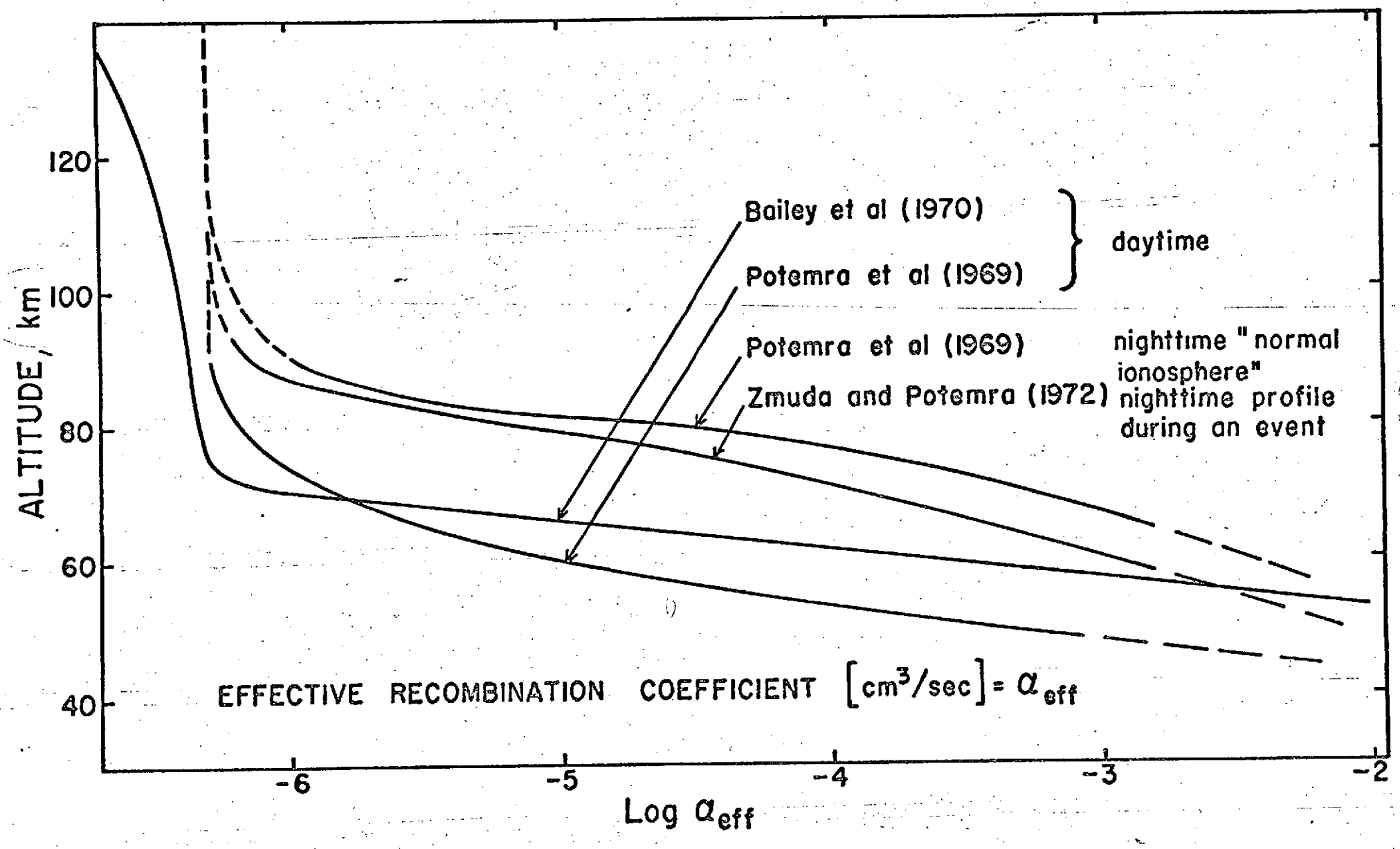
ALTITUDE, km
120
100
80
60
40
-6
-5
-4
-3
-2
Log α_{eff}
EFFECTIVE RECOMBINATION COEFFICIENT $[cm^3/sec] = \alpha_{eff}$
Bailey et al (1970)
Potemra et al (1969)
daytime
Potemra et al (1969)
Zmuda and Potemra (1972)
nighttime "normal ionosphere"
nighttime profile during an event

Fig. 4

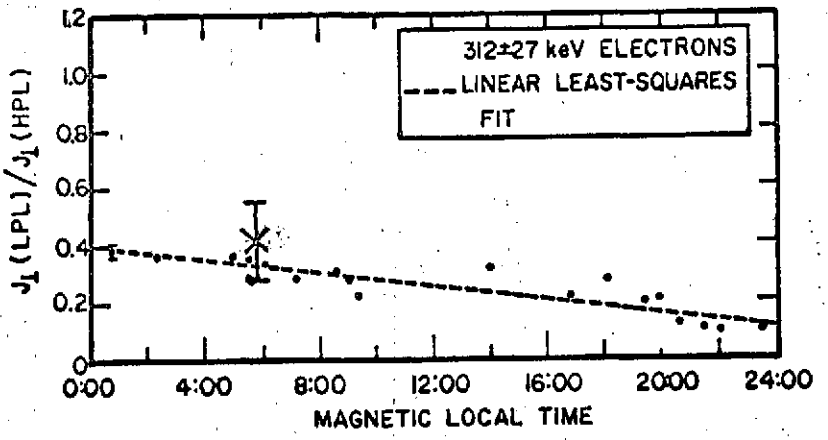
312±27 keV ELECTRONS
LINEAR LEAST-SQUARES FIT
$J_1(LPL)/J_1(HPL)$
1.2
1.0
0.8
0.6
0.4
0.2
0
0:00
4:00
8:00
12:00
16:00
20:00
24:00
MAGNETIC LOCAL TIME

Fig. 5

ANGULAR DISTRIBUTIONS OF SOLAR PROTONS AND ELECTRONS

E. NIELSEN and M. A. POMERANTZ
Bartol Research Foundation of The Franklin Institute
Swarthmore, Pennsylvania

and

H. I. WEST, JR.
Lawrence Radiation Laboratory, University of California
Livermore, California 94550

Abstract - High angular-resolution measurements of directional fluxes of solar particles in space have been obtained with detectors aboard OGO-5 during the cosmic ray event of November 18, 1968. This is the only case on record for which sharply-defined directional observations of protons and electrons covering a wide rigidity range (0.3 MV to 1.5 GV) are available.

The satellite experiment provided data for determining pitch angle distributions with respect to the direction of the local interplanetary magnetic field lines during the lengthy highly anisotropic phase of the event. It was found that the unidirectional differential intensities $j(\theta)$ of 3- to 25-MeV protons varied in accordance with the relationship $j(\theta) = b_0 + b_1 \cos\theta + b_2 \cos^2\theta$, where b_0 and $b_1 \geq 0$, and b_2 is positive, zero or negative. Soon after onset, 79-266-keV electrons arriving from the direction of the sun displayed an anisotropic component with the intensity varying as $\cos\theta$. Later, a double-peaked distribution appeared at the lower energies, whereas the flux at the upper end of the range covered by the experiment became isotropic. These results have been interpreted in the

light of the temporal flux profiles and the state of the interplanetary medium.

The observation of the unusually large and long-lasting anisotropies lead to several conclusions including:

(1) if injection of the solar particles was instantaneous, the diffusion coefficient was either constant or increasing with distance from the sun;

(2) if the solar source emitted particles over an extended period, and there is evidence to that effect, there was weak scattering in the region between the sun and the earth and a strong scattering region beyond the earth's orbit;

(3) solar electrons were stored near the sun;

(4) the observed angular distribution of 200-MV protons in the magnetosheath was in good agreement with that deduced in an earlier analysis of polar orbiting satellite observations and trajectory calculations.

1. Introduction

Satellite observations have revealed several general features of solar flare particle fluxes (McCracken et al., 1970). One typical characteristic is that the flux is generally anisotropic. In view of the relevance of the angular distributions of these fluxes for the understanding of the role of the interplanetary magnetic field in controlling the propagation of charged particles, an investigation of the pitch angle distributions in interplanetary space of low-energy protons and electrons of solar origin would be of great interest. However, owing to the lack of suitable observations, this has not heretofore been feasible.

If no scattering occurred between the sun and the earth, the solar cosmic rays would propagate in a manner such as to conserve their magnetic moment (first adiabatic invariant), thereby producing strongly collimated fluxes at 1 AU. Since such strongly-collimated particle fluxes have not been observed, their angular distribution can be considered the signature of the combined effects of the diverging interplanetary magnetic field (imf) lines and scattering mechanisms in interplanetary space. Spatial fluctuations in the imf provide the governing scattering process (Kaiser, 1973), and thus the angular distribution yields information about the interplanetary magnetic field regime.

Theories of cosmic ray transport have been treated extensively in the literature (Jokipii, 1968, 1971, 1972; Roelof,

1968, 1969, 1974; Klimas and Sandri, 1971; Kaiser, 1973; Earl, 1973a and b). We shall not discuss these in detail, but note that because particle transport may depend strongly on magnetic rigidity, it is of obvious interest to analyze observations which cover a wide range of rigidities. Therefore, the solar flare on November 18, 1968, which produced relativistic solar cosmic rays as well as highly-anisotropic fluxes of low-energy protons and electrons is of special importance, in view of the fact that this is the only recorded event for which well defined directional intensity observations have been obtained for protons and electrons covering a wide rigidity range.

Since this particular chromospheric eruption attracted widespread interest, the World Data Center has issued a special data compilation (WDC-A, 1970). For the present purposes, it suffices to note that the Importance 1B flare near the west limb (N20°, W90°) commenced at 1026 UT. The onset of Hα emission coincided with a rapid increase in x-ray flux level, indicating that particle acceleration apparently occurred during the flash phase. The interplanetary disturbance which gave rise to a Sudden Impulse (SI) at 1630 UT on November 18 is probably a shock and is relevant in the analysis of the particle fluxes.

Although the angular distribution has been determined experimentally for relativistic solar cosmic rays (Figure 1) observed during a number of ground-level events or GLE (Duggal, et al., 1971; Maurer et al., 1973), no similar detailed investigations have been previously conducted for the lower-energy particles that are observed with spacecraft.

During the November 18, 1968, event, Orbiting Geophysical Observatory 5 (OGO-5) was operating in interplanetary space, measuring with high angular-resolution directional-fluxes of low-energy protons ($0.57 \leq T_p \leq 46$ MeV) and electrons ($79 \leq T_e \leq 1530$ keV).

The purpose of the present study is primarily to analyze OGO-5 data recorded during this event in order to determine the angular distributions around the direction of the imf lines at early times (the first 12 hours following onset of the particle event), when the satellite was outside the magnetosphere. Information to aid in the interpretation of the observed angular distributions is obtained by studying the temporal flux profile.

2. Experimental Considerations

A. Instrumentation

The low-energy proton and electron data were obtained by the Lawrence Livermore Laboratories (LLL) energetic-particle experiment on OGO-5 (West et al., 1969, 1973). Some of the pertinent aspects of the experiment that are relevant to the present investigation are summarized here. A schematic cross section of the instrument is shown in Figure 2, and its relevant characteristics are listed in Table 1.

In the interest of background rejection for the electron spectrometer, both the detectors for each energy channel (except the two lowest where the detectors must be fairly thick ($\sim$0.2 mm) to reduce electronic noise), and their corresponding background detectors, were designed with a thickness corresponding approxi-

mately to the range of an electron of the specified energy. Pulses representing the peak of the distribution are selected by pulse height analysis. This design reduces the number of background counts which are produced by bremsstrahlung, penetrating energetic protons and degraded electrons scattered off the spectrometer walls.

The proton telescope is located in the line of sight of the entrance aperture of the high field electron spectrometer. It comprises four detectors and two absorbers. The latter are included to increase the energy range covered by the instrument. The energy of a proton is determined by measuring the energy deposited in each detector that it penetrates, and through the logical analysis of the pulses from the detectors. The proton channels and the logic statement discriminator settings used in defining the energy channels pertinent to this investigation are specified in Table 1. Note in the discussion that proton channels P3, P4, P5 and P6 are often referred to in terms of their approximate mean energy 1, 3, 9 and 25 MeV. The instrument had two additional channels extending down to 100 keV. However, protons of non-solar origin in this energy range are often found in the magnetosheath and nearby upstream-wave region (Lin et al., 1974; West and Buck, 1974) and hence were eliminated from the present investigation.

The intense low-energy portion of the electron spectrum (<4 MeV) is prevented from reaching the telescope by the magnetic field in the electron spectrometer; also, the detectors are so thin that, usually, an electron cannot deposit enough energy

in the detectors to overcome the thresholds. The same argument holds for bremsstrahlung. The primary source of background is penetrating energetic protons. Background corrections for all of the particle detectors are made according to the procedure outlined by West (1972).

OGO-5 was sun-earth oriented, hence the experiment aperture had to be scanned relative to the stabilized spacecraft to obtain directional information. NASA provided a special scan platform mounted on one of the spacecraft booms which always pointed toward the earth; hence the experiment scanned so as to look perpendicular to the earth-satellite radius vector (note the bottom panel of Figure 3). The scan was $\pm$ 115 degrees at a normal rate of 3° per second but occasionally 1 1/2° per second (note that the longest data acquisition interval was 4.6 seconds so that the angular resolution was not too adversely affected by the scan rates). It is unfortunate, certainly for this investigation, that a more complete ($\pm$180 degrees) scan was not available.

Simultaneous magnetic field data were obtained with the UCLA triaxial fluxgate magnetometer (P. J. Coleman and C. T. Russell) on board OGO-5. Because the primary purposes of the data analyses reported here are to determine the angular distributions and to deduce their physical significance, it is essential that the magnetic field and particle observations were conducted simultaneously.

Maximum information about pitch-angle distributions can be deduced from measurements recorded during periods in which the plane of scan contained or nearly contained the direc-

tion of the magnetic field lines. On the other hand, when the scan was perpendicular to the field lines, only observations near 90° pitch angle were obtained. To exploit the instrument to the fullest extent for the present purposes, the satellite must be outside the magnetosphere at a position where the plane of scan contains the garden-hose field line. During the 3 1/2 year lifetime of OGO-5, these conditions were satisfied only during the GLE on November 18, 1968.

The relevant part of the orbit of OGO-5 from 0200 UT on November 18, 1968 to 1500 UT on November 19, 1968, is shown in the upper panel of Figure 3. The bottom panel shows how the experiment aperture was scanning at the start of the measurements. Figure 4 shows the time profile of the magnitude, and longitude and latitude in Geocentric Solar Ecliptic (GSE) coordinates, of the observed magnetic field vector. These observations are used to determine the location of the bow shock and the magnetopause.

B. State of the Interplanetary Medium

During this event, Durney et al. (1972) and Quenby et al. (1974) observed the interplanetary magnetic field on the sunward side of the bow shock with Explorer 35. Their measurements indicated a rapid change in the direction of the imf at about 1630 UT, following which there was a decrease in the magnetic field intensity at OGO-5 which was in the magnetosheath during the interval 1600-2100 UT (Figure 4). At the same time (1630 UT) the geomagnetic field was perturbed, probably by a magnetohydrodynamic shock propagating in the solar wind, giving rise to a

Sudden Impulse (SI) recorded at low-latitude magnetic observatories (Kawasaki and Akasofu, 1970). After about 1800 UT the imf remained nearly aligned with the sun-earth line until 2400 UT.

We have indicated in Figure 3 the direction of the field $B_m^{(I)}$ in the magnetosheath which is tangential to the magnetopause. All points to the east of this line are magnetically connected to the sun, whereas all between it and the dusk and evening magnetopause are not. Also, particles propagating from the sun with trajectories on the sunward side of this tangential field line do not interact with the magnetosphere.

On the sunward side of the magnetic irregularity, between 2200-2400 UT, the average longitude of $\overline{B}_m$ is 55°, as indicated by $\overline{B}_m^{(II)}$ in Figure 3.

To illustrate the directions in which fluxes are measured, the look directions of the particle detectors are shown in Figure 5.

3. Intensity Variations

A. Measurements

Before presenting the observed temporal variations of the particle intensities and angular distributions a few points should be noted. It can be shown that adiabatic deceleration causes a maximum change in rigidity in the time interval of interest ($\sim$12 hours) which is less than 15% (Nielsen, 1974); hence, the effect of deceleration is insignificant and is not a cause of the phenomena to be discussed. Owing to the form of the energy spectra and the low velocity of the solar corpuscular

stream in the magnetosheath, it is evident that the corrections for convective effects (Forman, 1970; Balogh et al., 1973) are insignificant because of the large diffusive anisotropies encountered in this study; hence they have been ignored.

Figures 6 and 7 show J, the observed particle flux averaged over the plane of scan, plotted as a function of time for electrons and protons, respectively. In all figures displaying data points, the error bars represent twice the standard deviation of the mean, determined from a variance analysis, taking into account time variations of the flux. The intensity of 9- and 25-MeV protons and of the electrons increases rapidly to a maximum and then starts to decrease. At the time of arrival of the magnetic irregularity there is a decrease in counting rate in all the electron channels and in the 3- and 9-MeV proton channels, while the 25-MeV channel is affected less. There is a small maximum in the 79-keV electron flux at 1530 UT, while no indication of a maximum is observed at higher energies.

B. Analysis

Coherent Propagation. Earl (1973b) found that when the imf power spectrum is steep, a pulse of particles from a solar flare (the coherent pulse) may arrive at the orbit of the earth preceding the diffusing particles, thereby creating an initial flux maximum in the intensity profile. The Earl theory also treats the arrival of the initial group of particles predicting a propagation speed along the spiral interplanetary field $\geq$80% of the free propagation speed. Figure 8 shows the time-dependent arrival of the first particle fluxes in the various energy channels. The straight

line with slope-1 which best fits the data yields a total path of 1.74 AU. The Earl theory indicates a field-line length of ∿1.4 AU which is in accord with previous observations; Lin (1974) has reported ∿1.2 to 1.5 AU.

The maximum in the distribution (see Figures 6 and 7) predicted by coherent propagation should appear at $t'_m \leq 1.25/3\beta$ hr. following particle injection (here we have assumed a distance traveled of 1.5 AU, an upper limit of expectations). The observed time of maximum of 79-keV electrons is not inconsistent with the Earl theory, and hence the initial peak in this case would appear to be the result of scatter-free coherent propagation. For the other cases, excluding P3 for which the analysis is conclusive, the calculated times of maximum are too early to support a picture of coherent propagation alone.

Diffusive Propagation. Applying the theory of anisotropic diffusion with a boundary (ADB) of Burlaga (1967) to the proton measurements, as shown in Figure 9, we find that the data representing the intensity increase show a good fit to a straight line; this is in accordance with the theoretical prediction. We further find that the data corresponding to the early stages of the decay, similarly, are in accord with this model. From the slope of the curves in Figure 9, the time of maximum is determined to be 1513 UT and 1327 UT for 9- and 25-MeV protons, respectively, consistent with observations (Figure 7), and 1718 UT for 3-MeV protons. The smooth intensity profiles corresponding to the straight lines

in Figure 9 are plotted in Figure 7, to highlight the proton intensity variations caused by the magnetic irregularity (see Figure 4). Owing to short rise times and small intensity increases, a similar analysis of the electron and neutron monitor data was inconclusive.

The mean free paths, calculated using the Green's function solution to the diffusion equation for a spherically symmetric system with a point source at the sun, are found to be $\lambda_{\parallel}$ = 0.12, 0.11 and 0.12 AU for 3-, 9- and 25-MeV protons, respectively.

Associated Magnetic Field Intensity Variations. The sudden decrease in the proton and electron fluxes at 1530 UT (Figures 6 and 7) coincide with the sudden decrease in the magnetic field intensity, and is most likely caused by it. Because the magnetic flux through a cross-sectional area of a magnetic flux tube is constant ($\overline{\nabla}\cdot\overline{B}_i=0$), the observed decrease in the field intensity by a factor 2 (Figure 4) must produce a corresponding increase of the area, leading to a reduction of the particle flux inside the magnetic irregularity to half the flux outside. This is in accord with the observations. The decrease in J inside the magnetic irregularity is to some extent caused by the fact that only particles with pitch angles near 90° are detected there. Thus, owing to the restricted angular coverage, the angular distribution is undetermined.

Summary. It has been shown that the first peak in the proton flux can be described in terms of diffusion theory. If

the protons did diffuse from the sun toward the earth, the diffusion approximation, i.e. a first order approximation valid for small anisotropies, probably yields a realistic value of the mean free path which we have determined to be $\lambda_{\parallel} \sim 0.1$ AU. Early in an event the anisotropy is predicted to be large and to decay inversely with time (Fisk and Axford, 1969). In the early phase of the event under investigation the anisotropy remained large, ~100% (Section 4), and this may raise doubts about the validity of results obtained using the diffusion approximation. Early in an event the contribution of backscattered particles to the density is small, and thus of no governing influence upon the observed density. Absence of backscattered particles--i.e., persistent large anisotropies--possibly owing to a diffusion coefficient rapidly increasing with heliocentric distance, would therefore not seriously affect the cosmic ray density. If the cosmic rays in fact are diffusing between the sun and the earth the observed density would thus fit the diffusion equation to yield a mean free path which is a good approximation of the conditions at heliocentric distances < 1 AU.

Furthermore, the time of maximum flux in the 79-keV electron channel and the time of arrival of these electrons

are in line with expectations based upon the theory of coherent propagation.

It was also found that the intensity of 79-keV electrons exhibits a small secondary maximum at about 1530 UT, i.e., coincident with the detection of the magnetic irregularity. We will discuss these results later after presenting the angular distributions in the next section.

4. Angular Distributions

A. Measurements

The angular flux distributions around the direction of the observed magnetic field of both low-energy protons and electrons have been determined as they change owing to spatial and temporal effects.

The shock propagating from the solar direction stretches out the magnetic field lines in the region of space it has traversed causing weaker magnetic scattering behind compared with the region ahead, and this may account in part for the observed long duration of the large proton and electron anisotropies.

Protons. Representative angular distributions of protons are shown in Figure 10. At 1335 UT (i.e. at a distance of 700 Earth Radii (R_E) ahead of the magnetic discontinuity) the intensities of 3- to 25-MeV protons vary over the angular interval where the flux is measurable according to

$$j(\mu) = b_0+b_1\mu+b_2\mu^2. \qquad (1)$$

A statistical analysis indicates, with a 95% confidence level, that for the 3-MeV proton flux $b_2=0$, while at 25 MeV $b_2 < 0$. Thus, the angular distribution is energy dependent in the interval 3- to 25-MeV. Owing to the lack of information about the magnetic field configuration in the magnetosheath, a theoretical investigation of the distributions is not feasible.

Durney et al. (1972) utilized observations of 100-MeV (400 MV) protons made by a polar orbiting satellite together with trajectory calculations to deduce their angular distribution in interplanetary space at early times during the event of November 18, 1968. This result is shown in Figure 11 together with our observation of the distribution of 25-MeV (200 MV) protons. The angular distributions of protons with rigidities of 200 MV and 400 MV, both represent conditions shortly after onset of the event, and in view of the small difference in rigidities, the good agreement indicated in the figure constitutes heretofore unavailable evidence supporting the validity of the trajectory calculations.

Figure 12 shows the proton angular distributions observed within $\sim$300 R_E earthward of the magnetic discontinuity. The most striking features are the minima near 90°, with a

linear distribution for positive μ and a small maximum in the distribution for $\mu \simeq -0.4$. This pattern is clearly displayed by 25-MeV protons, but is barely discernible in the distributions of 3- to 9-MeV protons. The angular coverage is limited inside the magnetic irregularity, hence the results there are inconclusive.

An angular distribution representative of the observations on the sunward side of the tangential discontinuity for all energies is shown in Figure 13a. It is consistent with an exponential representation. However, owing to the statistical spread of the data points only a second order term in an expansion in cos θ can be determined.

At $\sim$2230 UT for 25 MeV and at $\sim$2230 UT for 3- and 9-MeV protons the angular distributions change into a superposition of an isotropic component upon an anisotropic component which is linear in μ for $\mu \gtrsim 0$ only (Figure 13b). At the same time the intensity of the isotropic component starts to increase rapidly, leading to a reduction of the anisotropy as the satellite approaches the magnetopause, and culminating in a nearly isotropic proton distribution in the magnetosphere near the magnetopause.

Electrons. Representative distributions of 79-keV electrons are shown in Figure 14, where (a) is the angular variation in directional fluxes at early times, i.e. $\lesssim$45 minutes following onset, and (b) illustrates the features at later times. In both cases the intensities for $\mu > 0$ are linear in cos θ. A

statistical analysis reveals that, while the distribution of the backscattered flux ($\mu < 0$) at later times (b) is independent of θ, at early times (a) the intensity decreases with cos θ. Similar results are obtained for the 158-keV and 266-keV electron flux, although in these cases the transition to a constant backscattered flux occurs earlier.

The temporal variation of the electron anisotropy is shown in Figure 15. For 79-keV electrons it is characterized by a gradual decrease with time, while at higher energies there is a pattern of an initial fast decrease (during 100 minutes after onset) followed by a nearly constant anisotropy until the arrival of the magnetic irregularity, when the anisotropy becomes indeterminate owing to the limited angular coverage.

Figure 16 shows several representative distributions obtained during the time interval 2200-2400 UT, when (1) the satellite is $\gtrsim 3\ R_E$ from the magnetopause, (2) magnetic field measurements are available and (3) the angular coverage is adequate. Figure 16a reveals a statistically significant bi-directional anisotropy in the 79-keV electron flux. The 158-keV electrons (b) seem to exhibit the same behavior though less pronounced, while at 266 keV the electron flux is isotropic.

B. Discussion

Protons. The observed proton distributions inescapably exhibit one common feature, namely that the anisotropy invariably is very large. The solar protons appear to be steadily streaming past the orbit of the earth; but even after this has continued

for 12 hours, hardly any flux propagating in the opposite direction along the field is detected.

The analysis shows that at least 4 hours elapse after onset before the proton flux from the antisolar direction rises above background. Hence the diffusion mean free path, $\lambda_{\parallel}$, of protons propagating parallel to the direction of the mean imf beyond the orbit of the earth, appears to be at least half the distance traveled in 4 hours, i.e. $\lambda_{\parallel}$ for 3-, 9- and 25-MeV derived this way is $\sim$1.2, 1.9 and 3.4 AU, respectively. McCracken et al. (1967) using similar arguments, found for some events $\lambda_{\parallel}$-values up to 2.7 AU for 10-MeV protons. However, Jokipii (1968) argued that an estimate of $\lambda_{\parallel}$ on this basis leads to an erroneous result.

In the theory it is envisaged that any net change in pitch angle is a sum of many small angle changes, and the time required to produce a backscattered flux propagating upstream along the field lines thus depends critically on the variation of scattering rate with pitch angle. Because $<(\Delta\mu)^2>/\Delta t$ is small around $\theta=90°$ it may take an exceedingly long time for particles to be scattered through 90°, thereby giving rise to large backscattering times ($\sim$4 hours as mentioned above). However, the diffusion mean free path $\lambda_{\parallel}$ is governed by the scattering in the region $0 < \theta < 90°$, and thus it is misleading to directly associate $\lambda_{\parallel}$ with the backscattering time.

Jokipii finds that the mean free path, calculated on the basis of the backscattering time, is roughly an order of magnitude larger than the diffusion mean free path deduced from the

intensity-vs-time profile. Thus, we find $\lambda_{\parallel} \sim 0(0.1\ AU)$. Jones et al. (1973) found that the diffusion coefficient near $\theta=90°$ is substantially different from zero, giving rise to a considerable scattering rate. In view of the controversy over the rate of scattering of particles with pitch angle near 90°, we conclude that the magnitude of the diffusion mean free path of protons beyond the orbit of the earth lies between the approximate limits 0.1 AU and 1 AU. The mean free path during this event was calculated for 1 MeV protons by Quenby et al. (1974) using magnetic field power spectra. They find $\lambda_{\parallel}$ determined in this manner to be a factor ∿12 smaller than the value deduced from the observed time-lapse between event onset and rise above background of the flux from the antisolar direction, a result that is in line with our findings.

Electrons. The solar-electron angular distributions exhibit two dominant features. Superposed upon an isotropic flux is an anisotropic component with pitch angles that do not exceed 90°, and for which the intensity is proportional to cos θ. Thus, while part of the electron population is isotropic, there is also a steady flow of electrons past the orbit of the earth, a situation which is not characteristic of diffusive propagation.

One possible explanation of the form of this distribution is that the electrons are weakly scattered in the region between the sun and the earth, whereas at larger distances from the sun the scattering probability increases, giving rise to the isotropic component. However, it is not necessary to invoke the effects of a distant scattering region in order to interpret these observations; one may, instead, ascribe the isotropic component to large-angle scattering of the electrons out of the collimated beam.

Earl (1973a) found that the angular distribution in the case of coherent propagation should be relatively uniform over the forward hemisphere. However, the effect of the diverging nature of the interplanetary field was not included in the calculations, and thus an observed distribution might be expected to be more collimated than the theory predicts. It should be noted that while the temporal profile of only the 79-keV flux could be interpreted in terms of coherent propagation, the angular distribution at that energy is similar to that observed at higher energies. Hence, the form of the measured angular distribution, per se, can not be regarded as supporting the coherent propagation model.

The initial rapid decrease of the electron anisotropy δ (Figure 15) is consistent with observations by Allum et al. (1971), who reported the results of a study of the anisotropies of electron fluxes during eighteen prompt solar-electron events that were observed by Explorer 35. They found that the anisotropies of $\geq$ 70-keV electrons were field aligned initially, with amplitudes generally ranging from 30-60% (the largest observed was 85%, July 30, 1967) that decayed to $\leq$10% within an hour or two. The fast decrease of δ for 158- and 266-keV electrons is a typical temporal feature of prompt electron events. However, the initial anisotropy in the present event is unusually large (90 to 100%) and is regarded as evidence of weak scattering.

Lin (1974) has noted that anisotropy measurements aboard earth-orbiting spacecraft may not reflect interplanetary conditions since $\sim 10^{-2}$ to 10 Hz waves of terrestrial origin (Fairfield, 1969; Russell et al., 1971) are commonly observed far upstream

from the earth's bow shocks. Since these waves seem to be associated with imf lines that connect to the bow shock they are far more probably on the dawn side of the earth than on the dusk side. It is not likely that these waves affected the present results, but if they are efficient in scattering the low-energy electrons we observed, this would most likely imply that the angular distributions are more collimated in interplanetary space than at the point of observation. Thus, confirmation of this effect would lend further evidence to the concept of weak scattering in interplanetary space.

Figure 15 shows that the anisotropy does not die away within one to two hours as Allum et al. (1971) found to be characteristic in the usual case. However, these authors reported observations made during one event, on October 30, 1967, which deviated from the typical pattern in a manner similar to the present one. That event displayed the following features: (1) a double-peak structure with a minimum at almost 0330 UT appeared in the temporal flux profile following onset at ∿0030 UT; (2) the anisotropy exceeded >30% for three hours following the onset of the electron increase; (3) a sudden impulse (SI) was observed at 0426 UT (Solar and Geophysical Data, 1967). The variation in the H-component as a typical low-latitude magnetometer station (Tangerang) was +35γ for the November 18 event, whereas on October 30, 1967, the SI-magnitude was +45γ. Thus, these two electron events share three features in common which may have their origin in the presence of a hydromagnetic shock in interplanetary space that gives rise to the sudden impulse.

At later times in the OGO-5 data, a second maximum in the angular distribution appears, denoting a flow of electrons from the antisolar direction centered on the magnetic field vector. The 79-keV electron flux is observed to remain anisotropic for about 12 hours.

Bi-directional anisotropies have previously been observed only for low-energy protons in so-called Energetic Storm Particle (ESP) events (Rao et al., 1967), and it is therefore of interest to see if the present bi-directional electron anisotropy can be interpreted in these terms. Such an event consists of particles swept up by a blastwave propagating in interplanetary space. Some of the particles leak out of the blastwave to produce anisotropic fluxes propagating both toward and away from the sun.

The gyroradius of a 260-keV electron in a 5-γ field is $\sim$0.08 R_E. The radius of curvature of the imf lines observed around 1630 UT is approximately 20 R_E, so in the absence of small-scale magnetic irregularities, the electrons could pass adiabatically through the "kink". Though a small maximum in the 79-keV electron flux is observed near the time of the arrival of the shock, the profile in this case does not have the characteristics determined for proton ESP-events, namely an abruptly increasing and decreasing intensity phase and a total duration of approximately six hours. Furthermore, we might expect a blastwave to be most effective in "sweeping up" particles which are slow compared to its speed, in which case the

characteristics of an ESP-event in the detected low-velocity protons as well as in the electron flux would be observed. However, no proton intensity increases occurred at this time (around 1630 UT). This suggests that the interpretation of the bi-directional anisotropy of the low-energy electrons as a manifestation of the mechanism discussed by Rao et al. (1967) is not applicable in the present case.

The maximum from the solar direction in the observed bi-directional anisotropies, may indicate that the flux of 79-keV solar electrons remained anisotropic throughout the entire period covered by our observations (i.e ∿14 hours following onset of the flare).

To account for these observations, which are in sharp contrast with the general pattern of prompt solar-electron events as reported by Allum et al. (1971), it appears to be necessary to assume storage of the observed low-energy electrons near the sun (Simnett, 1971, 1973). Since 266-keV electrons become isotropic before 79-keV electrons, the storage time for the latter is longer.

Summary. Considering the backscatter time we estimate that the mean free path of protons propagating beyond the orbit of earth lies between the approximate limits of 0.1 and 1 AU. The long-lasting large anisotropies can be seen, at least in part, as a consequence of the weak magnetic scattering in interplanetary space. Even weak scattering will eventually isotropize the flux, hence it is not necessary to invoke any additional

mechanisms in order to account for the fact that the solar cosmic rays eventually become isotropic. However, we should note that our observations are also qualitatively consistent with the presence of a diffusive region located at a distance beyond the orbit of the earth (Roelof, 1974). In this model, cosmic rays suffer only little or no scattering between the sun and the earth, and diffusion does not set in until the particles reach the distant scattering region, where the isotropic component near the earth's orbit has its origin. The electron observations are in good accord with the predictions of this model; the proton results, although inconclusive, are not inconsistent. To maintain long-lasting large field-aligned proton anisotropies at the orbit of the earth in the case of weak scattering in the inner solar system it would, however, be necessary for the solar-proton source to remain active over an extended time interval. Otherwise, in the case of both instantaneous injection and scatter-free propagation, the space within the earth's orbit would soon be emptied of particles propagating directly from the sun.

5. Conclusions

We have presented detailed observations of the angular distributions of low-energy protons and electrons during the early phase of the solar-particle event of November 18, 1968. The results and conclusions are as follows:

1) The protons displayed very large (nearly 100%) anisotropy, and the electron anisotropy was unusually large and long lasting.

2) The mean free path $\lambda_{\parallel}$ of 3-, 9- and 25-MeV protons propagating beyond the orbit of the earth was between ~0.1 AU and 1 AU; $\lambda_{\parallel}$ for protons propagating from the sun to the earth, as deduced from the time profile of the observed intensity, was ~0.1 AU. For instantaneous injection, this indicates that the diffusion coefficient was either constant or increasing with distance from the sun.

3) If it is assumed that the solar source was emitting particles over an extended period (i.e. not instantaneous injection), then our observations of angular distributions are consistent with the existence of weak scattering in the region between the sun and the earth and of a strong-scattering region located beyond the orbit of the earth.

4) From the unusually long duration of electron anisotropies we have inferred that the solar electrons were stored near the sun.

5) A field-aligned bi-directional anisotropy in the 79-keV electron flux was observed at late times. This phenomenon may be associated with the proximity of the magnetosphere at the time of observation.

6) Good agreement was found between the angular distribution of 200-MV (~25 MeV) protons observed in the magnetosheath and that of 400-MV (~100 MeV) protons deduced from observations made by a polar-orbiting satellite together with trajectory calculations (Durney et al., 1972), supporting the validity of these trajectory calculations.

Acknowledgments - We are grateful to S. P. Duggal and E. H. Levy for many helpful discussions. This research was supported by NASA Grant NGR 39-005-105.

Table 1: Relevant characteristics of Lawrence Livermore Laboratories energetic-particle experiment aboard OGO-5. The logic statement is exemplified as follows: the expression $D_1(1.35)[\overline{D_1(5.4)}+\overline{D_2(0.53)}]$ requires for an output that the signal in D_1 be greater than 1.35 MeV and, in the brackets that the signal in D_1 be not greater than 5.4 MeV or the signal in D_2 be not greater than 0.53 MeV.

	Channel symbol	Energy	Geometric factor cm^2-keV-str	Logic statement discriminator settings
Electrons	E1	79±23 keV	0.180	
	E2	158±27	0.277	
	E3	266±36	0.390	
	E4	479±52	0.605	
	E5	822±185	4.43	
	E6	1530±260	8.57	
	P3	0.57-1.35 MeV	1.30×10^{-2}	$D_1(0.57)[\overline{D_1(1.35)}+\overline{D_2(0.53)}]$
	P4	1.35-5.40	1.30×10^{-2}	$D_1(1.35)[\overline{D_1(5.4)}+\overline{D_2(0.53)}]$
	P5	5.60-13.3	1.25×10^{-2}	$D_1(1.35)D_2(1.3)[\overline{D_1(5.8)}+\overline{D_2(5.7)}+\overline{D_3(0.2)}]$
	P6	14.0-46	1.72×10^{-2}	$D_2(0.5)D_3(1.2)[\overline{D_2(5.7)}+\overline{D_3(9.0)}+\overline{D_4(0.2)}]$
Omnidirectional proton measurement	O_2	>80 MeV		

Figure Captions

Fig. 1 Relativistic solar cosmic ray intensity measured with ground-based nucleonic intensity detectors. Results are expressed as percent of the galactic cosmic-ray background during an early epoch of the November 18, 1968 event and are plotted as a function of the cosine of the angle between the asymptotic direction of viewing (i.e., the direction from which the cosmic rays, causing an intensity increase at a given station, arrive at the boundary of the geomagnetic field) and the axis of symmetry in the angular flux distribution + is the centroid of data points, and the straight line connects it to the origin. The axis of symmetry is approximately parallel with the direction of the lines of force of the interplanetary magnetic field at the orbit of the earth (after Maurer et al., 1973). In the present paper, a similar analysis of low-energy-particle data, obtained in space with OGO-5 during the same event is carried out.

Fig. 2 The high-energy electron spectrometer and proton telescope. Here we show only one of the 180° first-order-focusing spectrometers comprising the electron-detection system (a second spectrometer provides four low-energy channels). Note that EB5, EB6 and EB7 are background channels. The proton telescope takes advantage of the electron spectrometer magnet to completely remove electron background.

Fig. 3 Experimental conditions. The Geocentric Solar Ecliptic (GSE) coordinate system is used in which $\overline{X}_{GSE}$ points toward the sun along the sun-earth line, and the $\overline{Z}_{GSE}$-axis points toward ecliptic north. $\overline{Y}_{GSE}$ is determined by the right hand rule. A part of OGO-5's trajectory on November 18-19, 1968, is constructed by rotating each point along the orbit into the ecliptic plane (i.e., the XY-plane) around the X-axis. The earth's bow shock and magnetopause are drawn through the points of observation at 0200 UT on November 18 and 0300 UT on November 19, respectively: $\overline{V}_w$ is the solar-wind velocity vector; its deflection upon crossing the bow shock is illustrated. $\overline{B}_m^I$ and $\overline{B}_m^{II}$ show the direction of the observed magnetic field averaged over the time intervals 1100-1530 UT and 2200-2400 UT, respectively. The bottom panel illustrates the satellite observational configuration; the elevation of which is 35°N at 1100 UT (November 18) and 21°N at 0300 UT (November 19).

Fig. 4 Magnetic field observations by OGO-5 from 1100 UT on November 18 to 0530 UT on November 19, 1968. θ_{min} is the minimum angle between any observed directional flux and the direction of the magnetic field. Between 1600 and 2130 UT, the angular coverage extends only to about $\pm$10° around the direction perpendicular to the magnetic field vector; this is insufficient for the determination of angular distributions. The flux of 3-MeV protons averaged over the plane of scan is also shown.

Fig. 5 The projections on the ecliptic plane of the directions in which fluxes are observed representative of the time interval (a) 1100-1700 UT and (b) 1700-2400 UT. The angle between the direction of observation and the ecliptic plane is indicated in each case.

Fig. 6 J, the directional electron fluxes averaged over the plane of scan, vs time. Mean directional intensities are also indicated. The vertical arrows indicate the time of maximum for 158-keV and 79-keV electron fluxes predicted by the theory of coherent propagation. The energies indicated are the appropriate mean energies for the channels.

Fig. 7 J, the directional proton fluxes averaged over the plane of scan, vs time. The dashed curves are constructed using the curves in Figure 9 and indicate diffusive propagation. The onset of 1-MeV protons is between 1600 and 2000 UT. The vertical arrows indicate the time of maximum predicted by the theory of coherent propagation. The energies indicated are the appropriate mean energies for the channels.

Fig. 8 $\beta = v/c$ vs the time interval between the onset of the flare at the sun and the onset of the particle event in the different energy channels. β is calculated for the upper energy limit in each channel, i.e. P6 (46 MeV), P5 (13.3 MeV), P4 (5.4 MeV), P3 (1.35 MeV), E1 (102 keV) and E2 (185 keV). Channel 01 responds to protons with energies >100 MeV as indicated by a vertical line. The

horizontal lines indicate the uncertainty in determining the onset times.

Fig. 9 Test for diffusive propagation in the ADB-model. J is the average of the directional proton fluxes in the plane of scan. The vertical arrows indicate the points which correspond to the observed times of maximum. Only two arrows are shown because the diffusion maximum in the flux of 3-MeV protons, as evident from Figure 7, is not observed owing to the influence of the magnetic irregularity.

Fig. 10 Directional proton fluxes vs cos θ. Here θ is the angle between the average magnetic field vector and the directions in which the flux is measured. The distributions in front of the shock are shown. Satisfactory statistical precision was achieved by averaging the particle measurements over the time intervals indicated in the figures.

Fig. 11 A comparison with proton measurements from other sources during the event. The data points and curve 1 are from Durney et al. (1972), and represent the angular distribution in interplanetary space of ∿100-MeV protons at 1115 UT on November 18, 1968, as determined from observations of polar-cap proton fluxes together with trajectory calculations. Curves 2 and 3 are the distributions of 25-MeV protons observed by OGO-5 in interplanetary space at 1210 UT and 1340 UT, respectively.

Fig. 12 Intensity vs cos θ at a distance of ~300 R_E in front of the propagating interplanetary shock. The data show a minimum in the angular distribution of 25-MeV protons in a direction nearly perpendicular to the direction of the mean magnetic field.

Fig. 13 Proton angular distributions behind the shock - (a) well away from the magnetopause and (b) as the satellite approaches the magnetopause.

Fig. 14 Angular distributions of electrons in front of the shock (a) shows that the directional flux intensity is decreasing as cos $\theta \rightarrow -1$ at early times following onset, while at later times, as illustrated in (b) and (c), the intensity is independent of direction when cos $\theta < 0$. At all times the distribution for cos $\theta > 0$ is linear in cos θ.

Fig. 15 Time variation of the electron anisotropy $\delta = (j_{max}-j_{min})/(j_{max}+j_{min})$.

Fig. 16 Angular distributions of electrons observed behind the interplanetary shock. A bi-directional field-aligned anisotropy is clearly displayed only at 79 keV.

References

Allum, F. R., Rao, U. R., McCracken, K. G., and Palmeira, R.A.R. (1971). Solar Phys. 17, 241.

Balogh, A., Webb, S., and Forman, M. A. (1973). Planet. Space Sci. 21, 1802.

Burlaga, L. F. (1967). J. Geophys. Res. 72, 4449.
Burlaga, L. F. (1969). Solar Phys. 7, 54.
Burlaga, L. F. (1971). J. Geophys. Res. 76, 4360.

Burlaga, L. F., and Ness, N. F. (1969). Solar Phys. 9, 467.

Duggal, S. P., Guidi, I., and Pomerantz, M. A. (1971). Solar Phys. 19, 234.

Durney, A. C., Morfill, G. E., and Quenby, J. J. (1972). J. Geophys. Res. 77, 3345.

Earl, J. A. (1973a). Astrophys. J. 180, 227.

Earl, J. A. (1973b). Technical Report 73-098, University of Maryland.

Fairfield, D. H. (1969). J. Geophys. Res. 74, 3541.

Fairfield, D. H. (1971). J. Geophys. Res. 76, 6700.

Fisk, L. A. and Axford, W. I. (1969). Solar Phys. 7, 486.

Forman, M. A. (1970). Planet. Space Sci. 18, 25.

Forman, M. A. (1971). J. Geophys. Res. 76, 759.

Jokipii, J. R. (1968). Astrophys. J. 152, 997.

Jokipii, J. R. (1971). Rev. Geophys. Space Phys. 9, 27.

Jokipii, J. R. (1972). Astrophys. J. 172, 319.

Jones, F. C., Kaiser, T. B., and Birmingham, T. J. (1973). Phys. Rev. Letters 31, 485.

Kaiser, T. B. (1973). Technical Report, No. 74-033, University of Maryland.

Kawasaki, K., and Akasofu, S.-I. (1970). WDC-A Report UAG-9, 92.

Klimas, A. J. and Sandri, G. (1971). Astrophys. J. 169, 41.

Lin, R. P. (1974). Space Sci. Rev. 16, 189.

Lin, R. P., Meng, C.-I., and Anderson, K. A. (1974). J. Geophys. Res. 79, 48.

Maurer, R. H., Duggal, S. P. and Pomerantz, M. A. (1973). J. Geophys. Res. 78, 29.

McCracken, K. G., Rao, U. R., and Bukata, R. P. (1967). J. Geophys. Res. 72, 4293.

McCracken, K. G., and Rao, U. R. (1970). Space Sci. Rev. 11, 155.

Nielsen, E. (1974). Ph.D. Thesis, Bartol Research Foundation, Thomas Jefferson Univ., July 1974.

Quenby, J. J., Morfill, G. E., and Durney, A. C. (1974). Planet. Space Sci. 21, 971.

Rao, U. R., McCracken, K. G., and Burlaga, R. P. (1967). J. Geophys. Res. 72, 4325.

Roelof, E. C. (1968). Can. J. Phys. 46, S990.

Roelof, E. C. (1969) in H. Ögelman and J. R. Wayland (eds.), Lectures in High-Energy Astrophysics, NASA Spec. Publ. 199, 199.

Roelof, E. C. (1974). EOS Trans. AGU 55, 386.

Russel, C. T., Childers, D. D., and Coleman, P. J. Jr. (1971). J. Geophys. Res. 76, 845.

Simnett, G. M. (1971). Solar Phys. 20, 448.

Simnett, G. M. (1973). IGPP-UCR-73-12, University of California, Riverside.

Solar Geophysical Data (1967). Principal Magnetic Storms.

Verzariu, P., and Krimigis, S. M. (1973). Planet. Space Sci. 21, 971.

West, H. I., Jr., Wujeck, J. H., McQuaid, J. H., Jenson, N. C., D'Arcy, R. G., Jr., Hill, R. W., and Bogdanowicz, R. M. (1969). Report UCRL-50572, University of California Lawrence Livermore Laboratory.

West, H. I., Jr. (1972). Report UCRL-51307, University of California Lawrence Livermore Laboratory.

West, H. I., Jr., Buck, R. H., and Walton, Jr. R. (1973). Report UCRL-51385, University of California Lawrence Livermore Laboratory.

West, H. I., Jr., and Buck, R. H. (1974). EOS Trans. AGU 55, 693.

World Data Center A (1970). Report UAG-9.

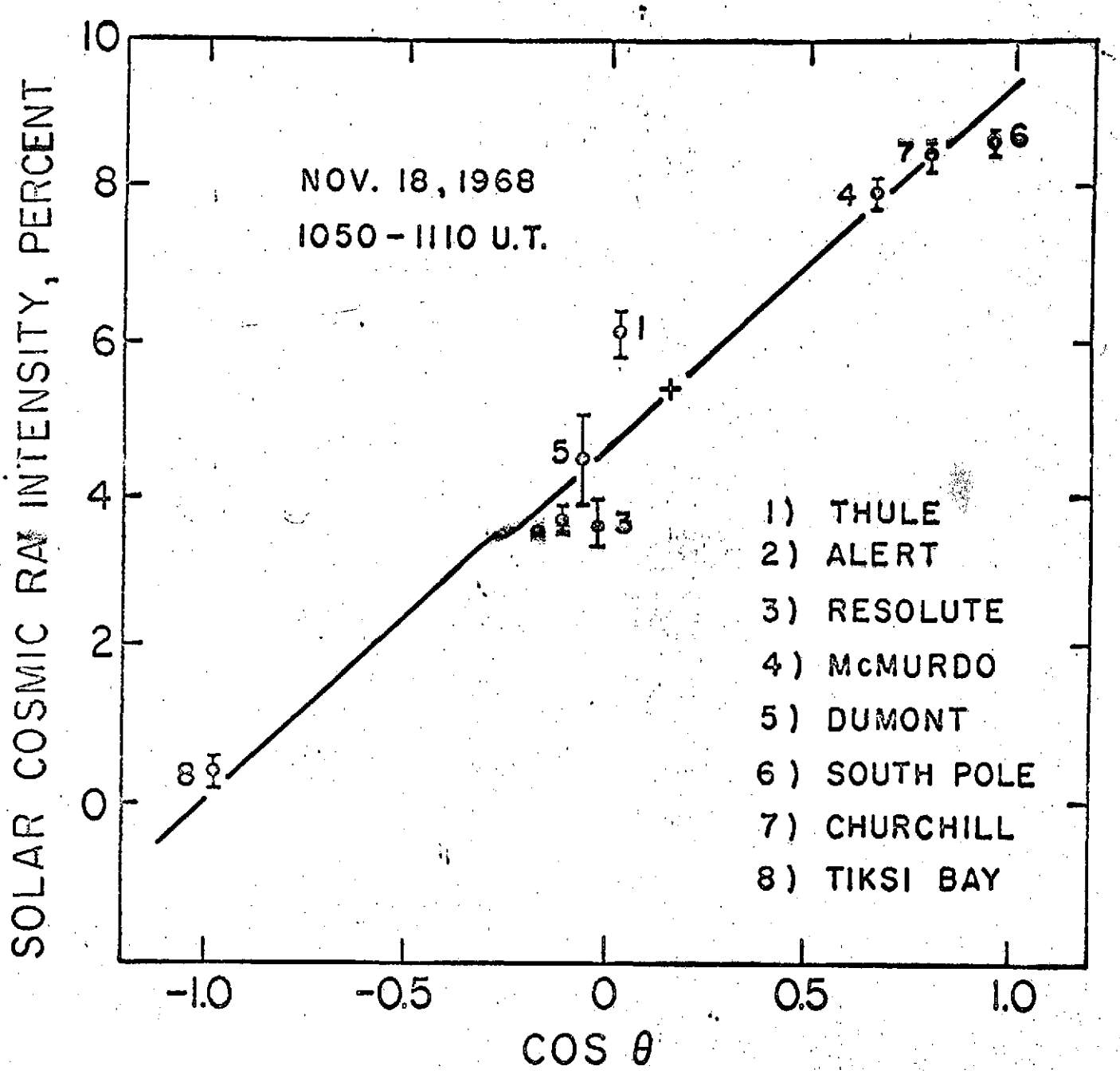
SOLAR COSMIC RAY INTENSITY, PERCENT
10
8
6
4
2
0
NOV. 18, 1968
1050 - 1110 U.T.
1) THULE
2) ALERT
3) RESOLUTE
4) McMURDO
5) DUMONT
6) SOUTH POLE
7) CHURCHILL
8) TIKSI BAY
-1.0
-0.5
0
0.5
1.0
COS θ

Figure 1

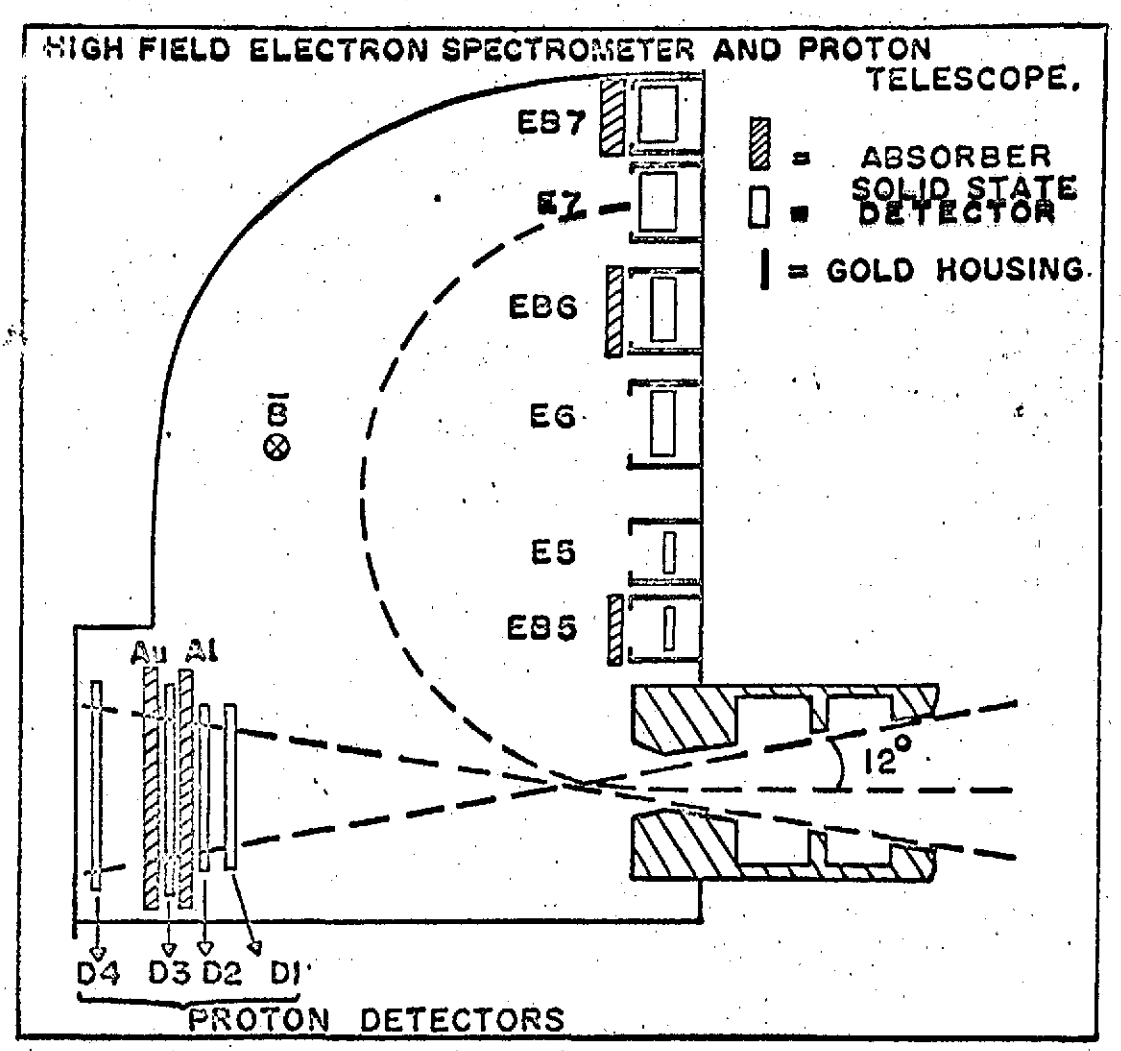
HIGH FIELD ELECTRON SPECTROMETER AND PROTON TELESCOPE.
EB7
E7
EB6
E6
E5
EB5
B
Au Al
12°
D4 D3 D2 D1
PROTON DETECTORS
= ABSORBER
= SOLID STATE DETECTOR
= GOLD HOUSING.

Figure 2

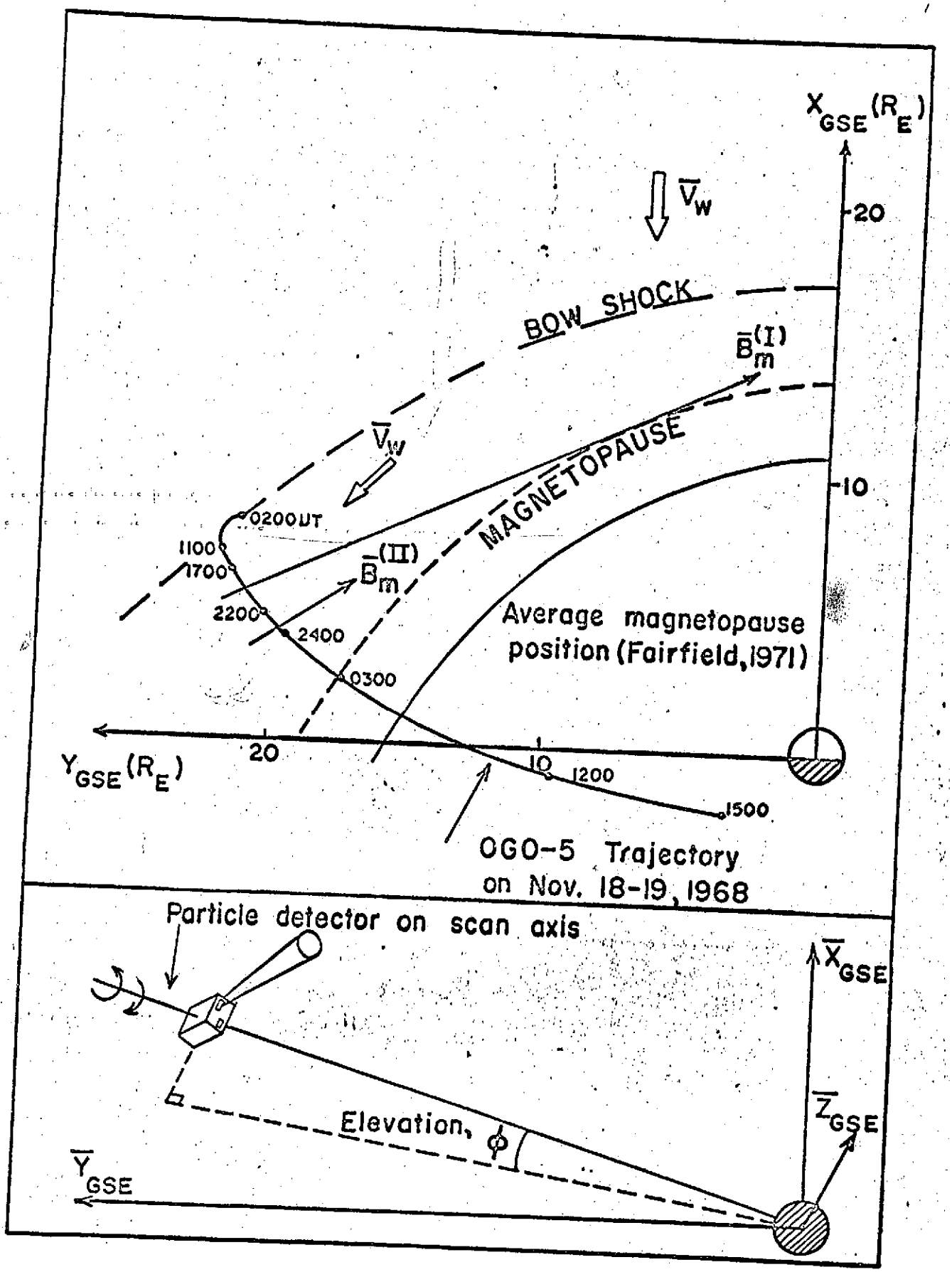
$X_{GSE}(R_E)$
$\bar{V}_W$
20
BOW SHOCK
$\bar{B}_m^{(I)}$
$\bar{V}_W$
MAGNETOPAUSE
10
0200UT
1100
1700
$\bar{B}_m^{(II)}$
2200
2400
0300
Average magnetopause position (Fairfield, 1971)
$Y_{GSE}(R_E)$
20
10
1200
1500
OGO-5 Trajectory on Nov. 18-19, 1968
Particle detector on scan axis
$\bar{X}_{GSE}$
$\bar{Z}_{GSE}$
Elevation, ϕ
$\bar{Y}_{GSE}$

Figure 3

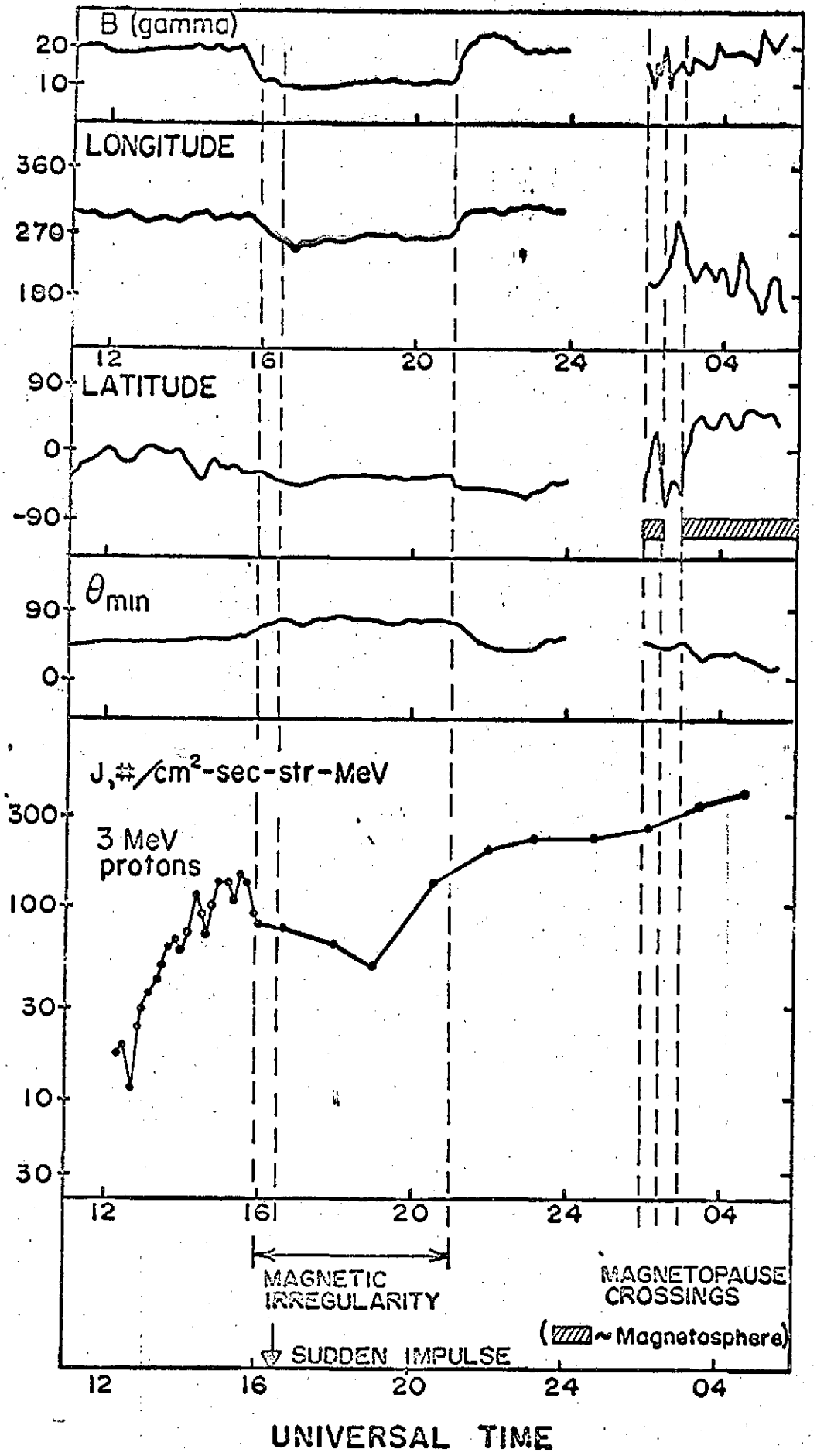
B (gamma)
20
10
LONGITUDE
360
270
180
12
16
20
24
04
90
LATITUDE
0
-90
θmin
90
0
J,#/cm²-sec-str-MeV
300
3 MeV
protons
100
30
10
30
12
16
20
24
04
MAGNETIC
IRREGULARITY
MAGNETOPAUSE
CROSSINGS
(~Magnetosphere)
SUDDEN IMPULSE
12
16
20
24
04
UNIVERSAL TIME

Figure 4

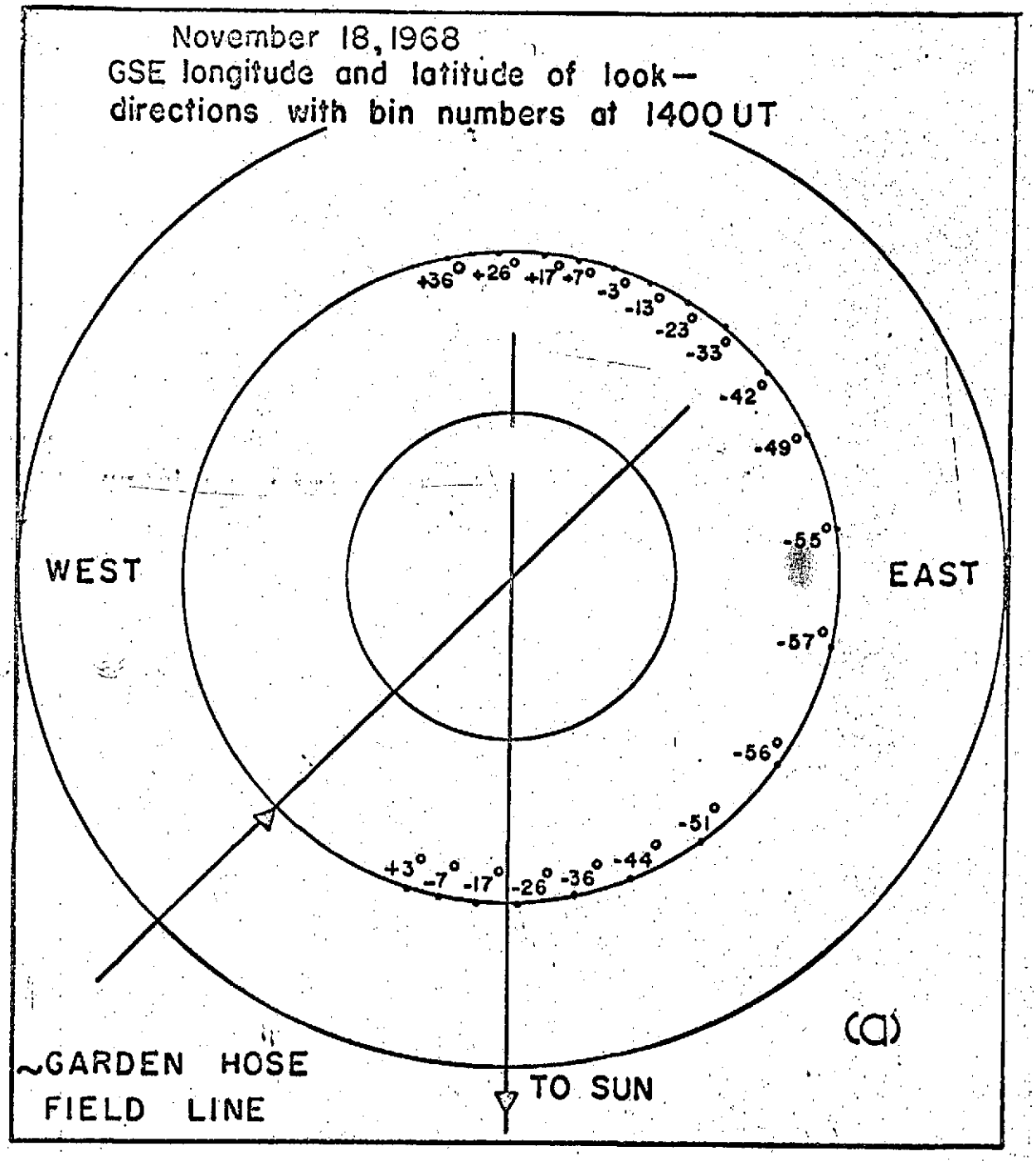
November 18, 1968
GSE longitude and latitude of look—
directions with bin numbers at 1400 UT
+36° +26° +17° +7° -3° -13° -23° -33° -42° -49° -55° -57° -56° -51° -44° -36° -26° -17° -7° +3°
WEST
EAST
(a)
~GARDEN HOSE
FIELD LINE
TO SUN

Figure 5 (a)

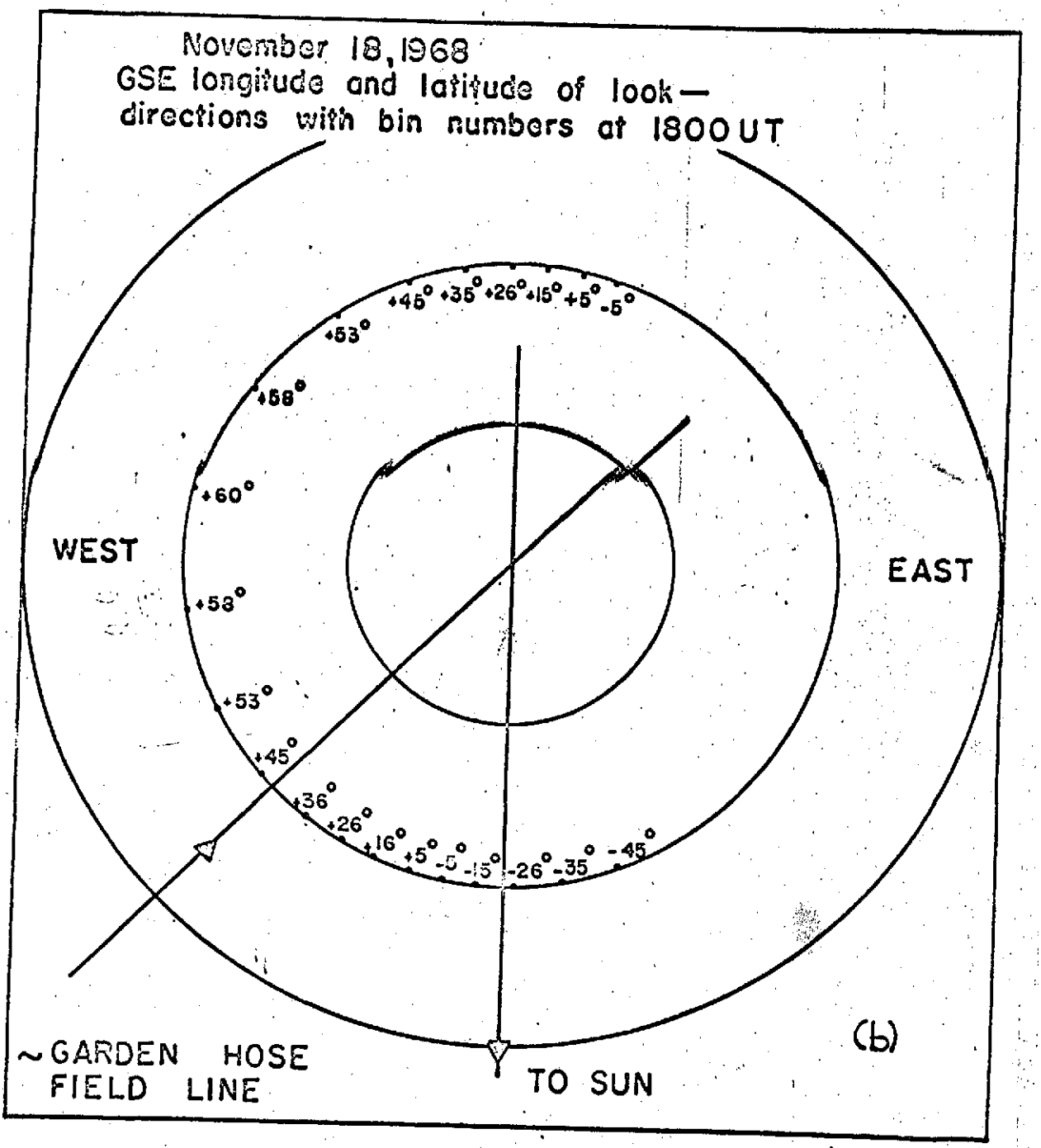
November 18, 1968
GSE longitude and latitude of look—
directions with bin numbers at 1800 UT
+45° +35° +26° +15° +5° -5°
+53°
+58°
+60°
WEST
EAST
+58°
+53°
+45°
+36°
+26°
+16°
+5°
-5°
-15°
-26°
-35°
-45°
(b)
~GARDEN HOSE
FIELD LINE
TO SUN

Figure 5 (b)

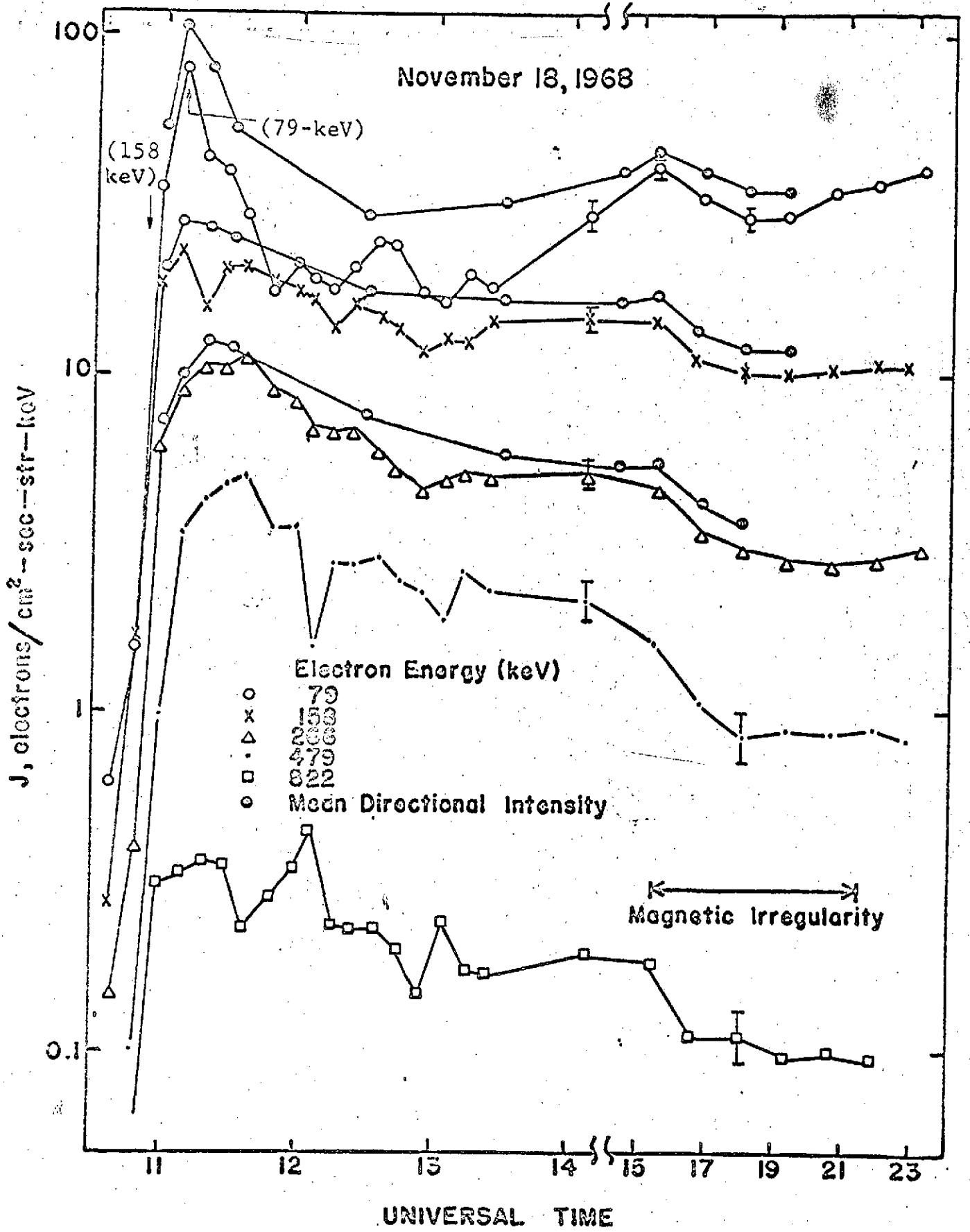
November 18, 1968
(79-keV)
(158 keV)
100
10
1
0.1
J, electrons/cm²-sec-str-keV
Electron Energy (keV)
79
153
206
479
822
Mean Directional Intensity
Magnetic Irregularity
11
12
13
14
15
17
19
21
23
UNIVERSAL TIME

Figure 6

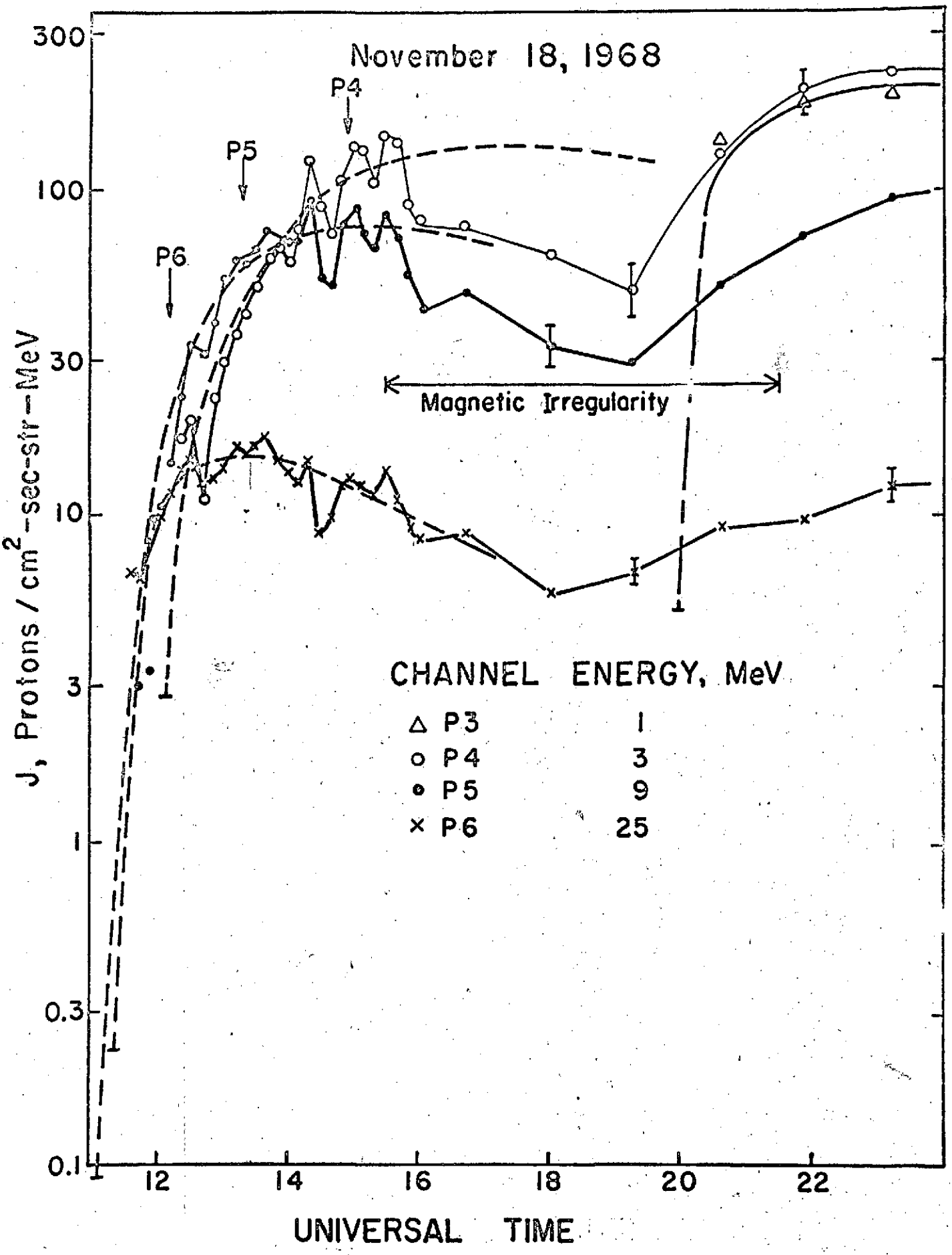
November 18, 1968
P4
P5
P6
Magnetic Irregularity
CHANNEL ENERGY, MeV
△ P3 1
○ P4 3
• P5 9
× P6 25
J, Protons / cm² - sec - str - MeV
300
100
30
10
3
1
0.3
0.1
12
14
16
18
20
22
UNIVERSAL TIME

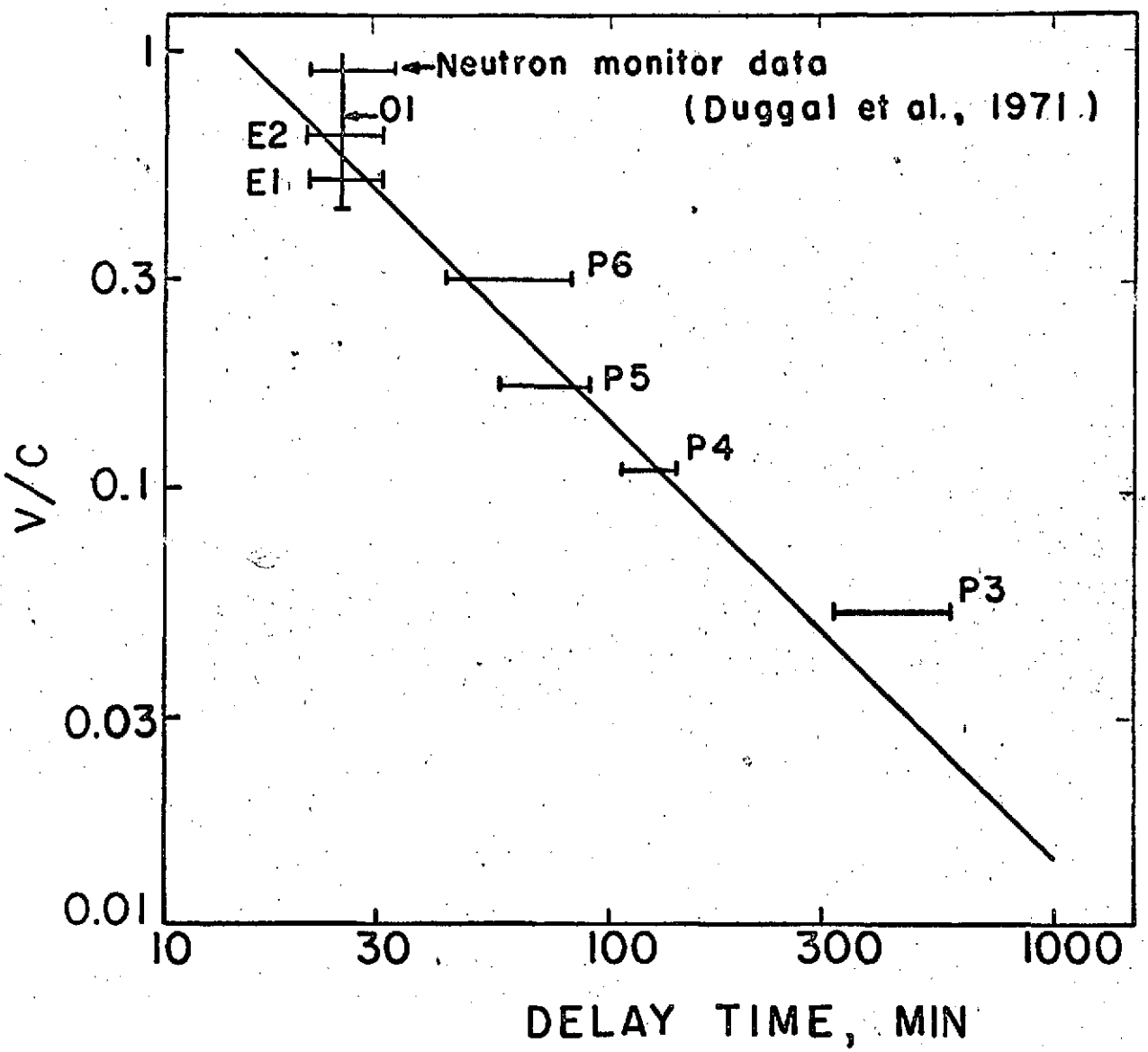
Neutron monitor data
(Duggal et al., 1971.)
O1
E2
E1
P6
P5
P4
P3
V/C
1
0.3
0.1
0.03
0.01
10
30
100
300
1000
DELAY TIME, MIN

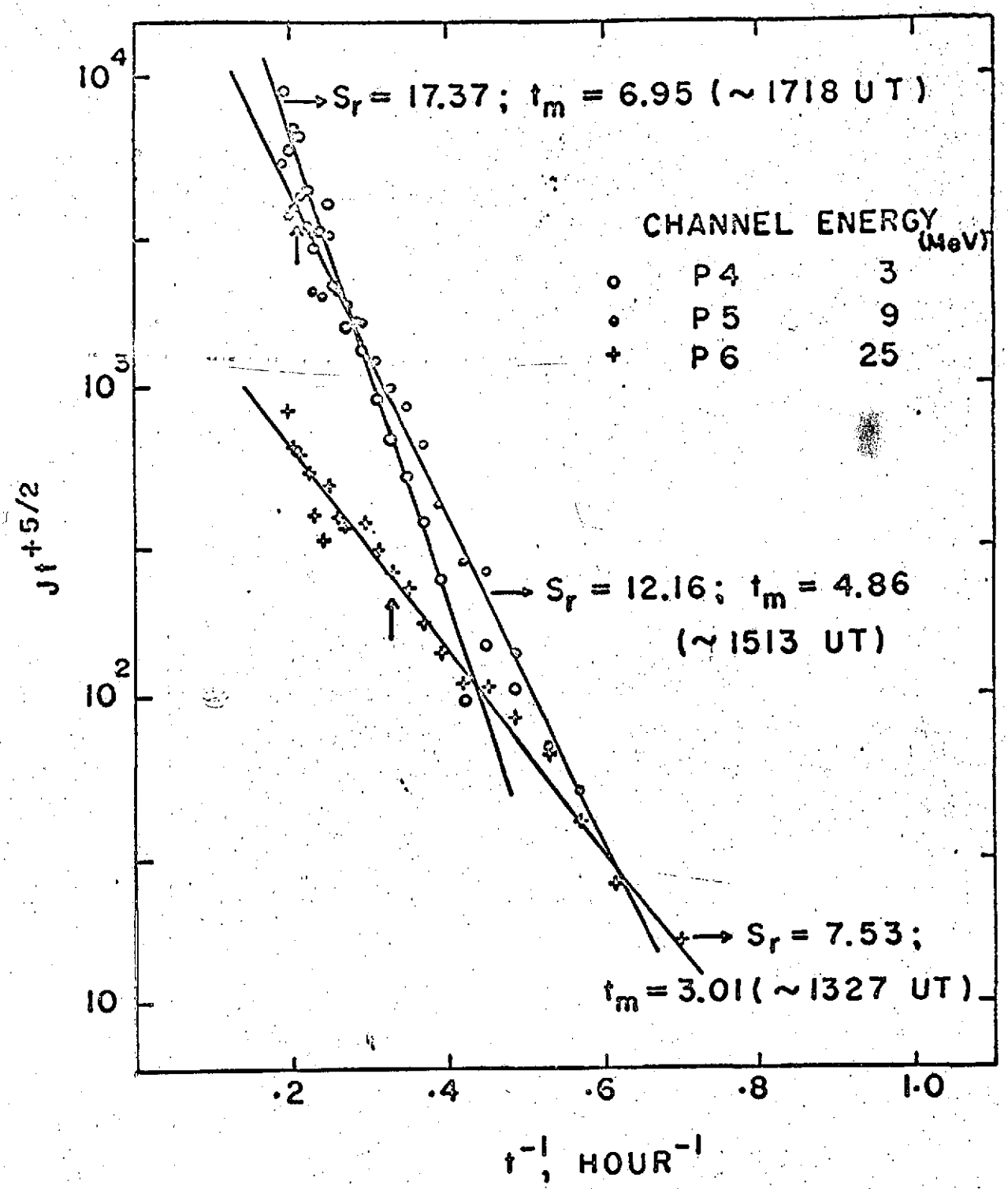
$S_r = 17.37$; $t_m = 6.95$ (~1718 UT)
CHANNEL ENERGY (MeV)
P4 3
P5 9
P6 25
$S_r = 12.16$; $t_m = 4.86$
(~1513 UT)
$S_r = 7.53$;
$t_m = 3.01$ (~1327 UT)
$Jt^{+5/2}$
10^4
10^3
10^2
10
.2
.4
.6
.8
1.0
t^{-1}, HOUR^{-1}

Figure 9

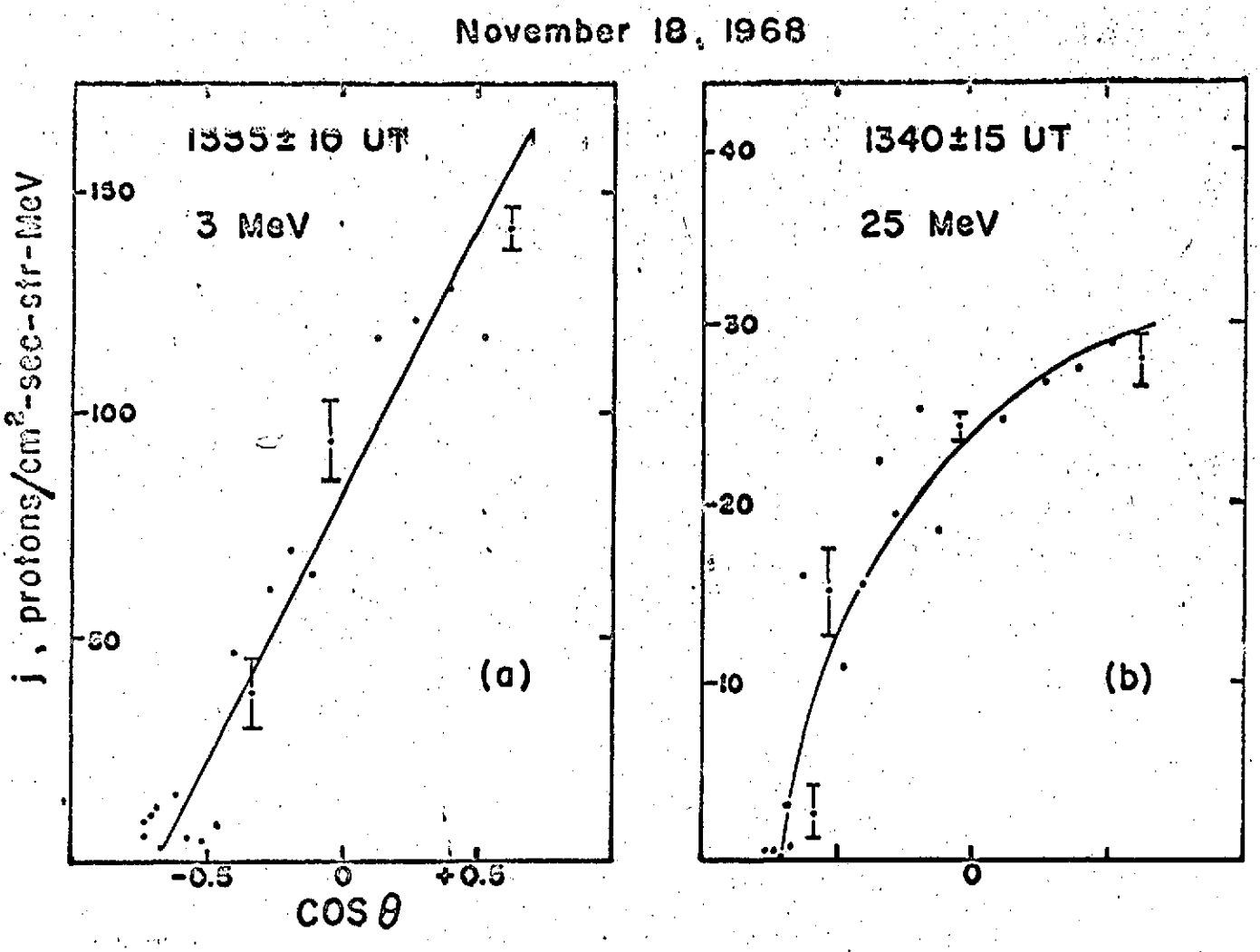
November 18, 1968
1355±16 UT
3 MeV
(a)
j, protons/cm²-sec-str-MeV
150
100
50
-0.5
0
+0.5
cos θ
1340±15 UT
25 MeV
(b)
40
30
20
10
0

Figure 10

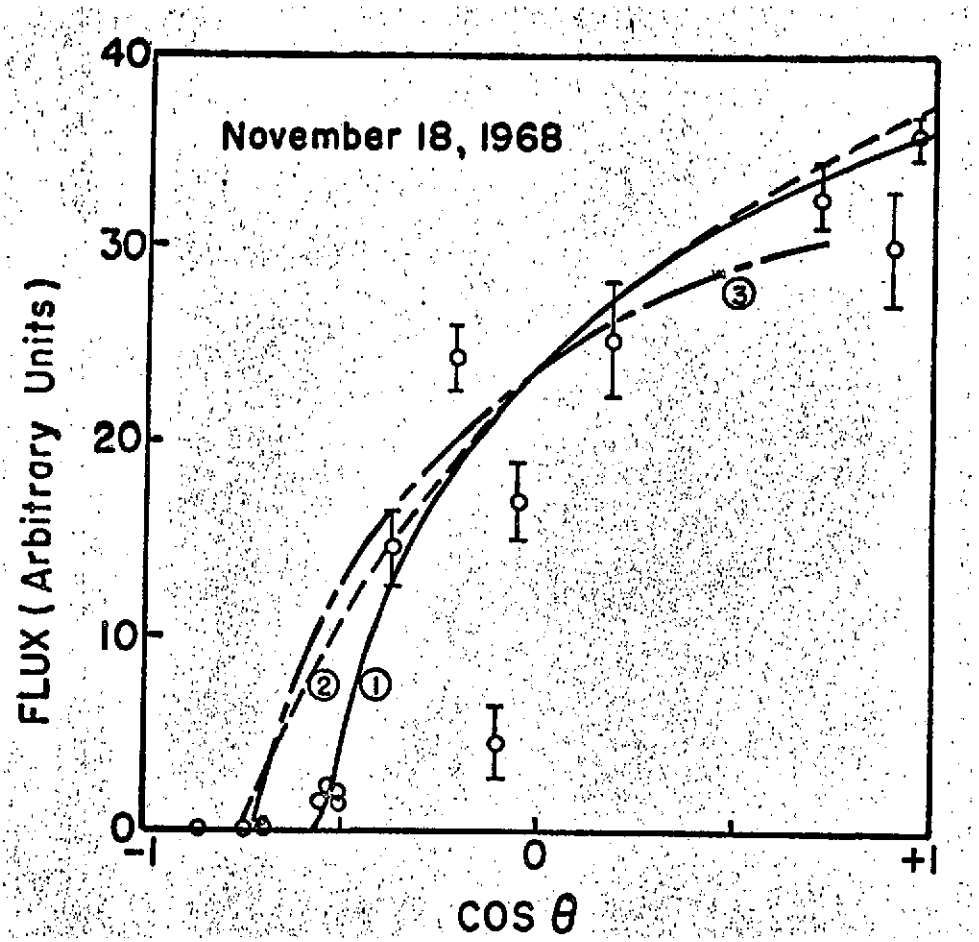
November 18, 1968
FLUX (Arbitrary Units)
40
30
20
10
0
-1
0
+1
cos θ
①
②
③

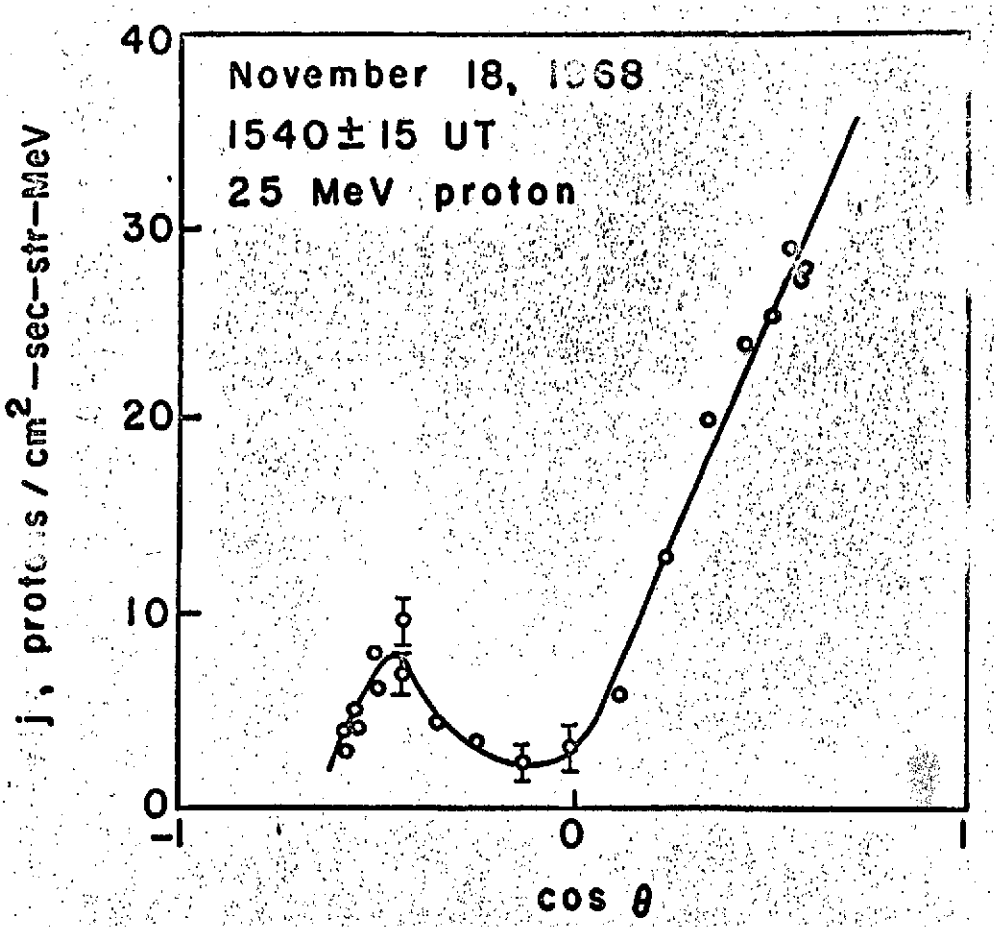
November 18, 1968
1540 ± 15 UT
25 MeV proton
40
30
20
10
0
-1
0
1
cos θ
j, protons / cm² - sec - str - MeV

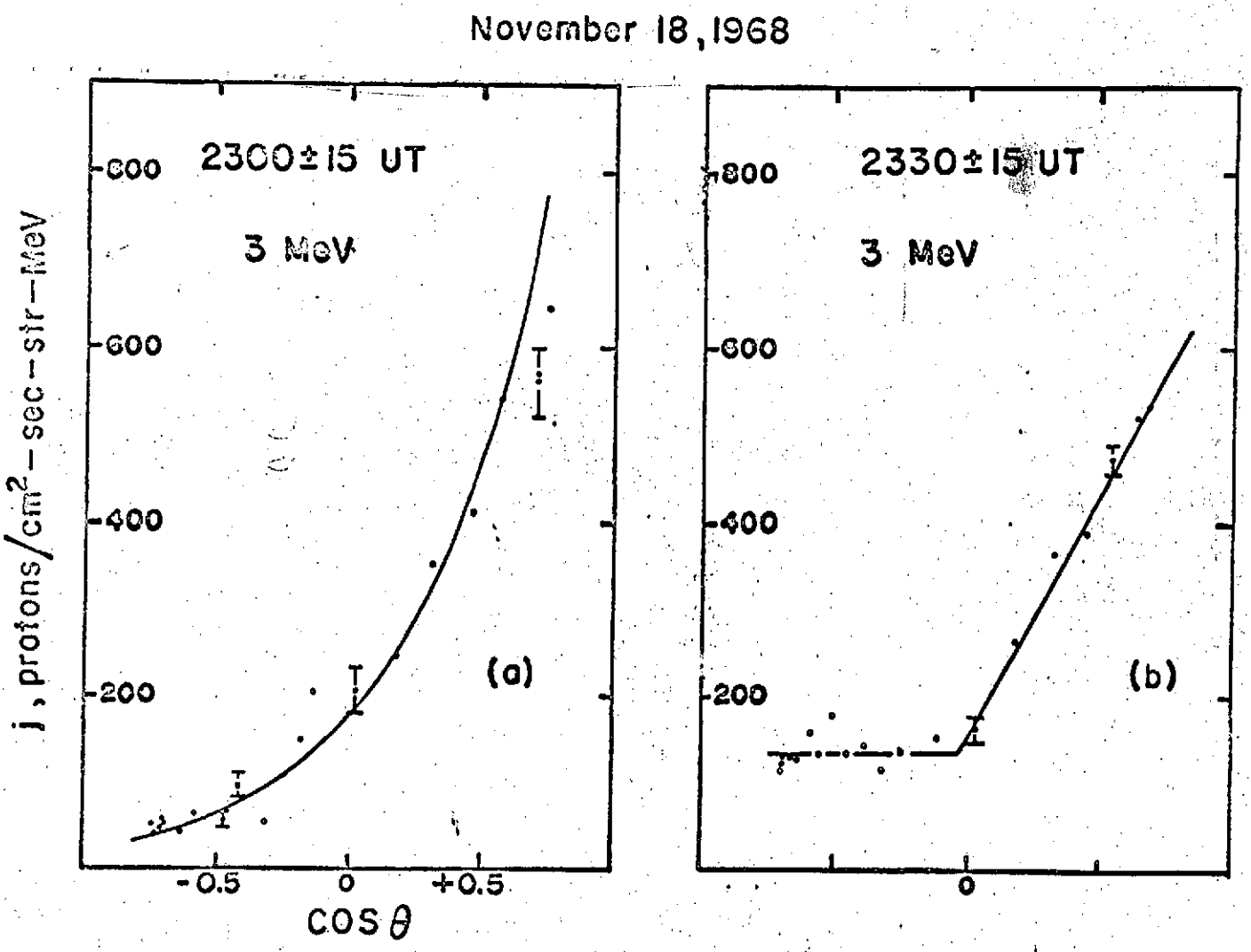
November 18, 1968
2300±15 UT
3 MeV
(a)
2330±15 UT
3 MeV
(b)
j, protons/cm²-sec-str-MeV
800
600
400
200
-0.5
0
+0.5
COS θ

Figure 13

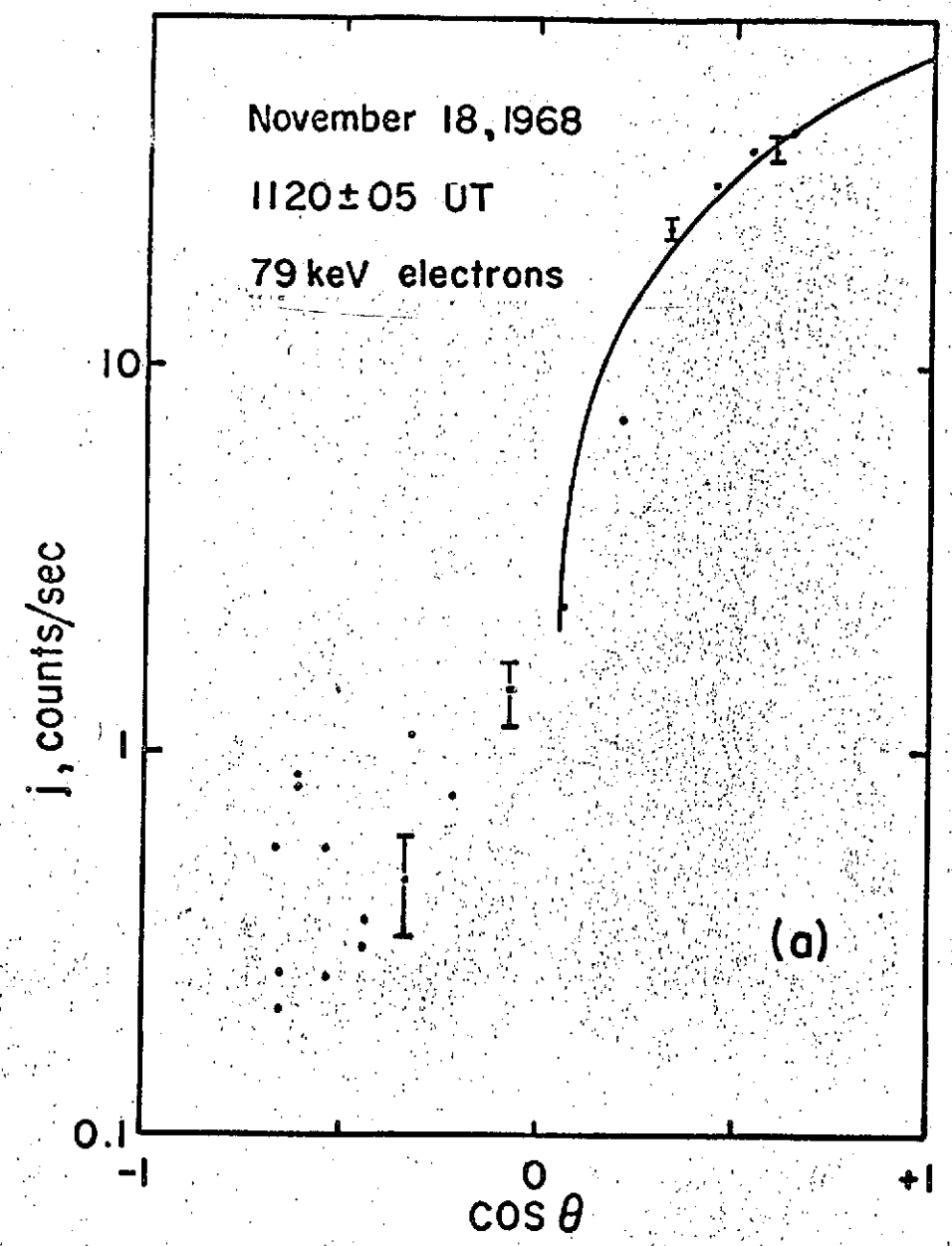
November 18, 1968
1120±05 UT
79 keV electrons
10
1
0.1
j, counts/sec
-1
0
+1
cos θ
(a)

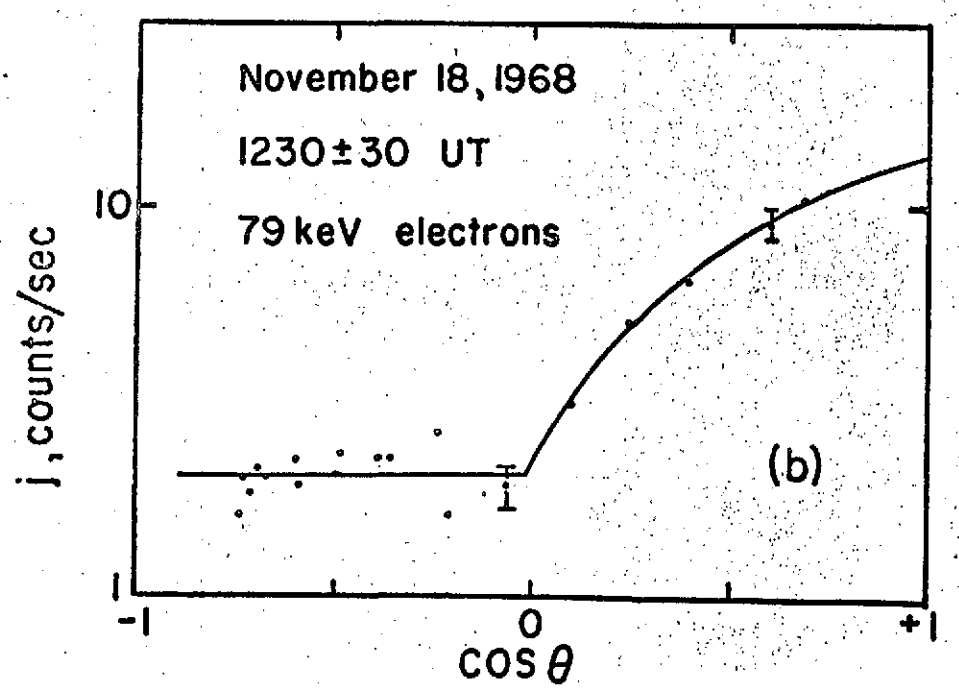
November 18, 1968
1230±30 UT
79 keV electrons
10
1
j, counts/sec
-1
0
+1
cos θ
(b)

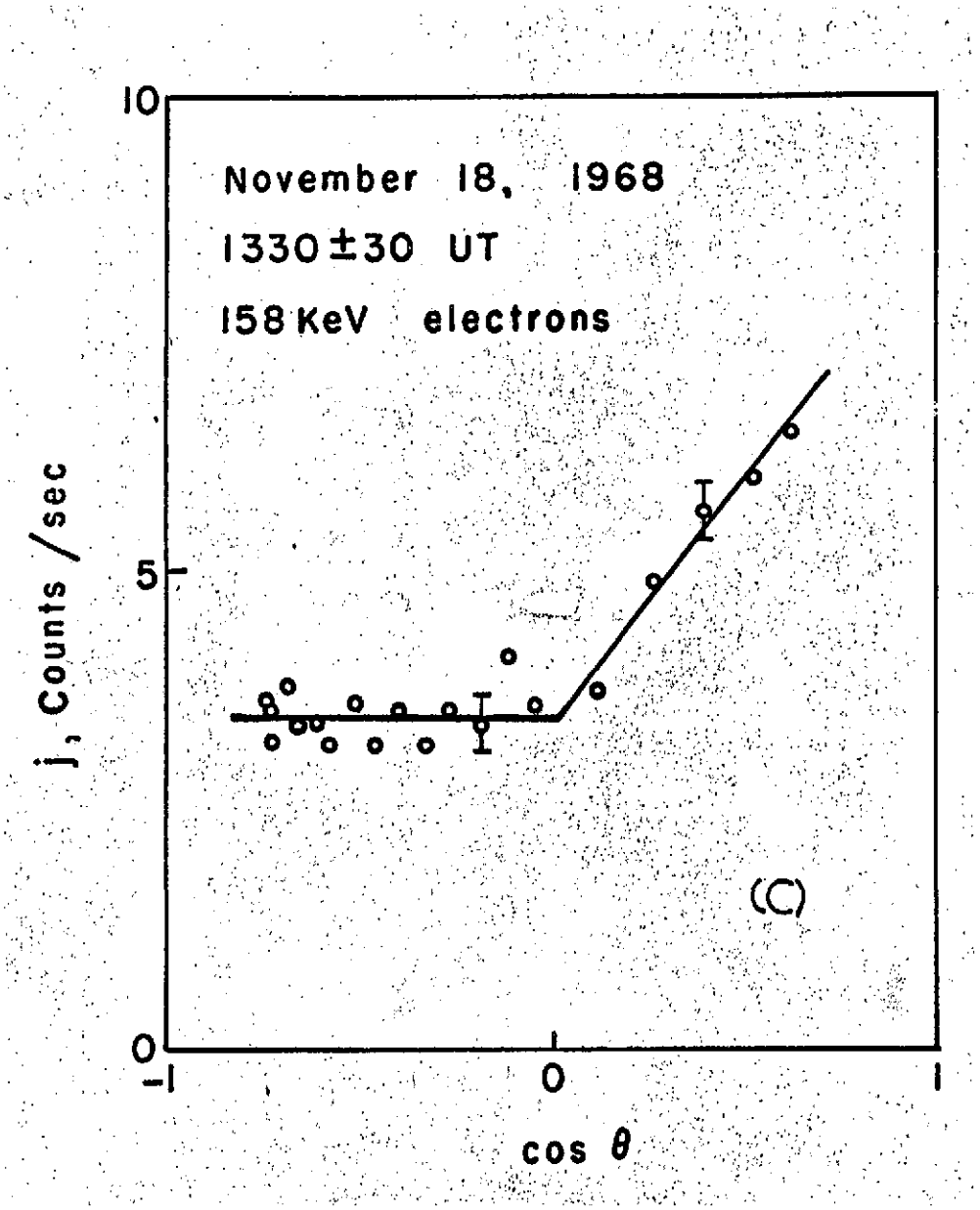
November 18, 1968
1330 ±30 UT
158 KeV electrons
(C)
j, Counts /sec
cos θ
10
5
0
-1
0
1

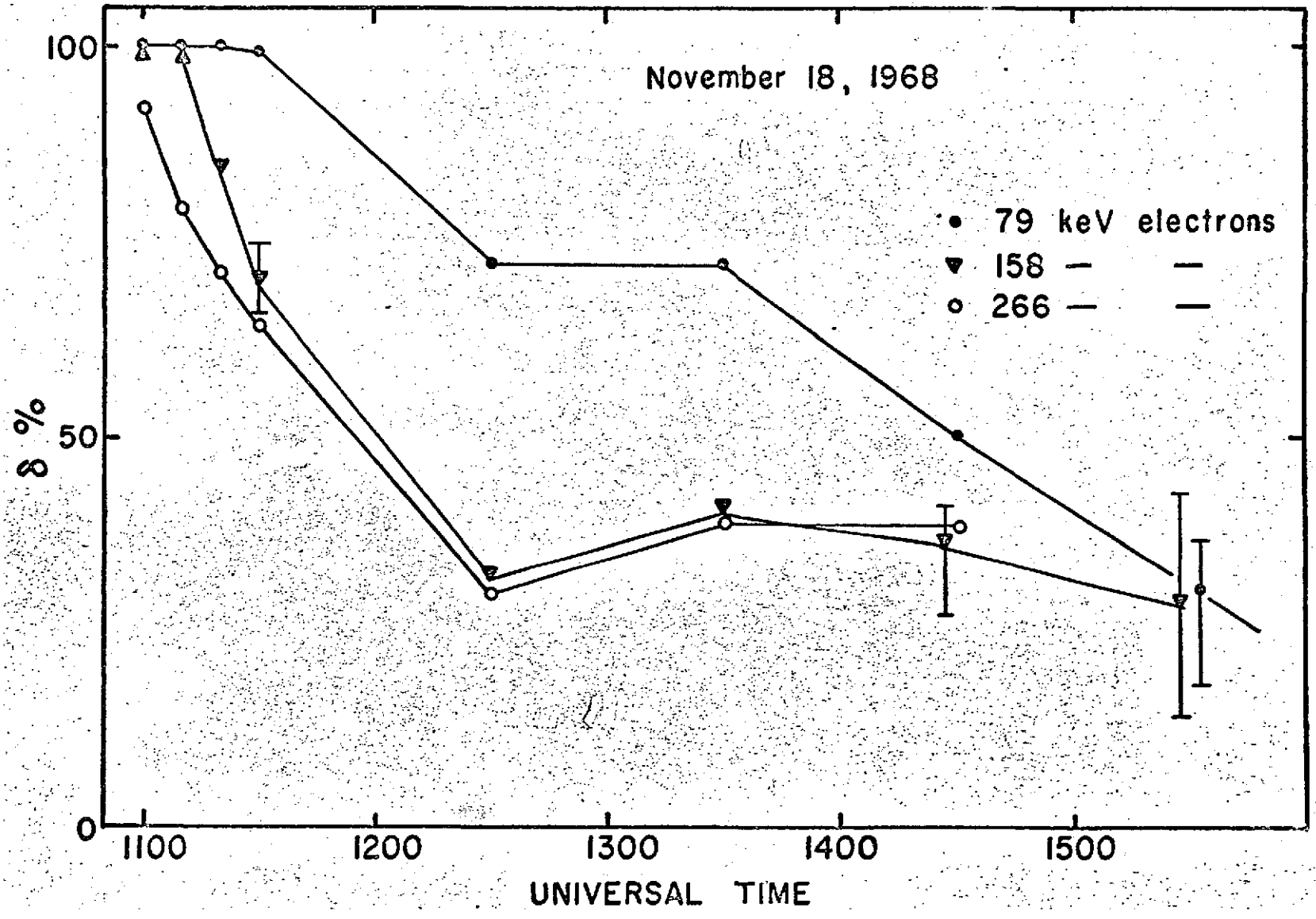
November 18, 1968
79 keV electrons
158 — —
266 — —
100
50
0
δ %
1100
1200
1300
1400
1500
UNIVERSAL TIME

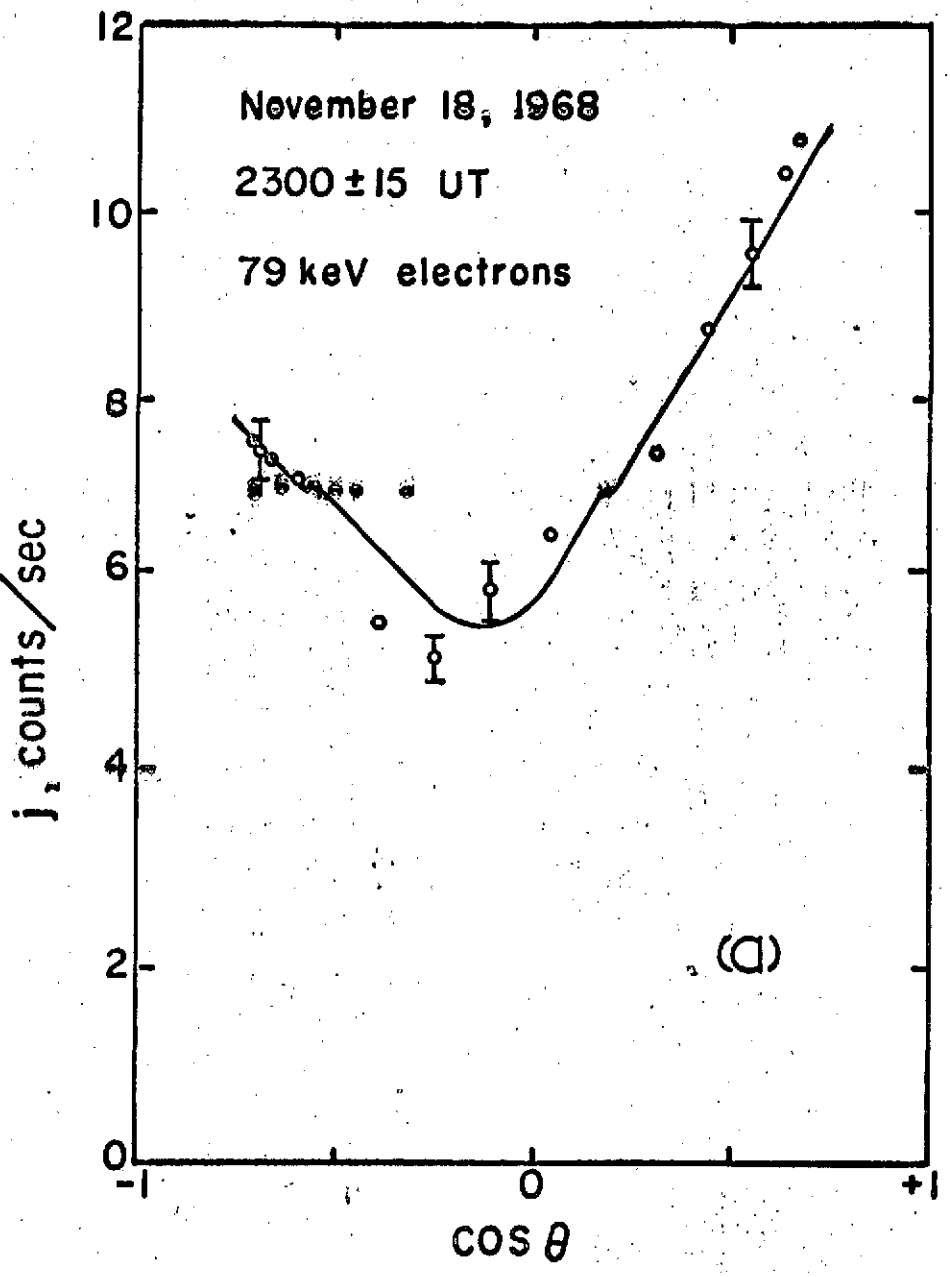
November 18, 1968
2300 ± 15 UT
79 keV electrons
(a)
12
10
8
6
4
2
0
-1
0
+1
j, counts/sec
cos θ

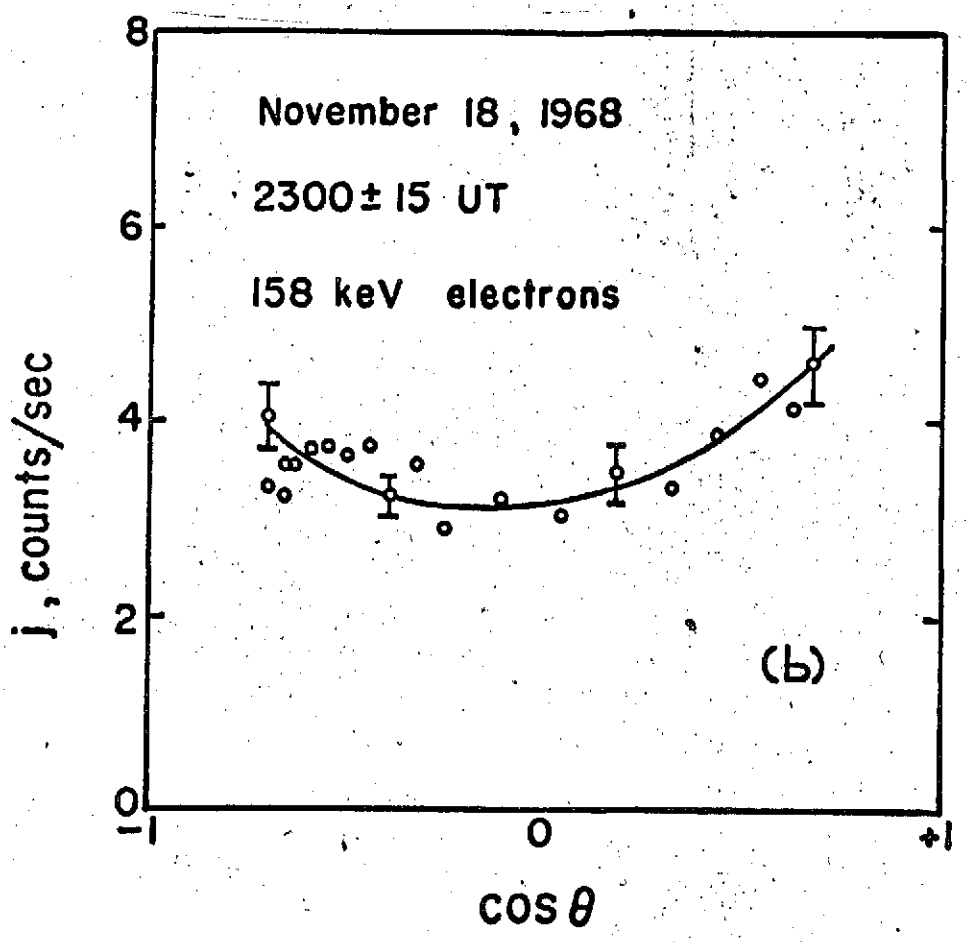
November 18, 1968
2300 ± 15 UT
158 keV electrons
(b)
j, counts/sec
cos θ
8
6
4
2
0
-1
0
+1

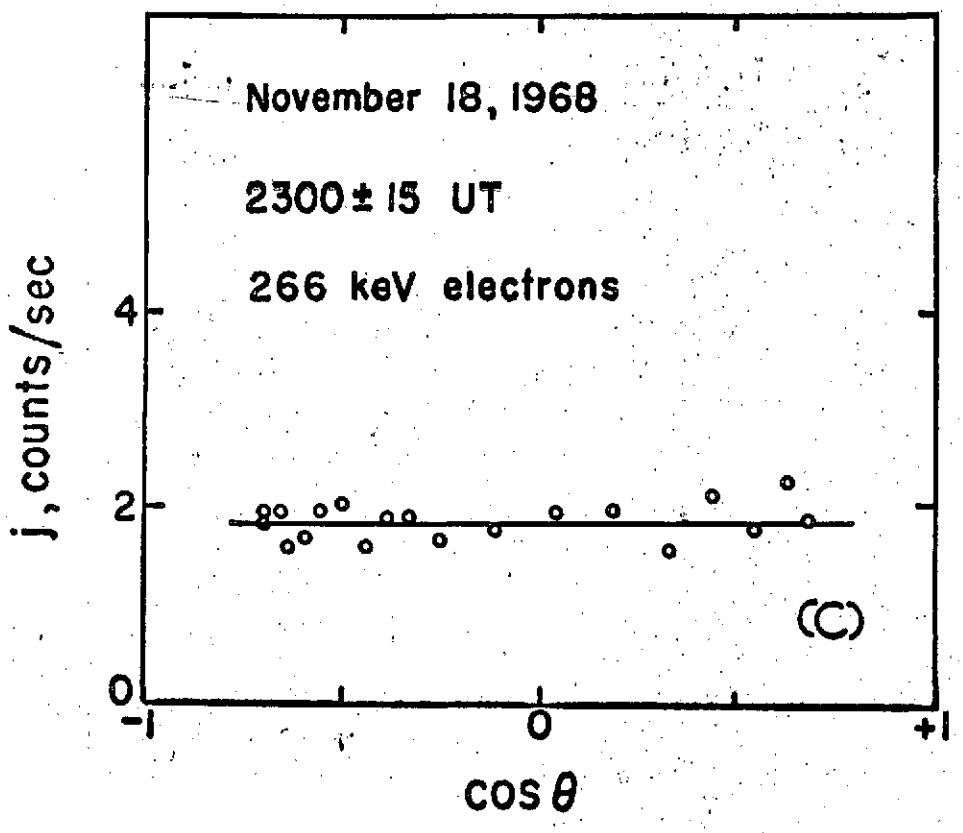
November 18, 1968
2300 ± 15 UT
266 keV electrons
(C)
j, counts/sec
0
2
4
-1
0
+1
cos θ